2018 CHOICE Award Winner
– Essential

Necessary title for librarians to have in their collection
on the forefront of the Remote Sensing industry.
Well written and stands out as the best in its field.

New in the Third Edition

- Includes updated EO missions, such as the new meteorological platforms (NPP and NOAA-20), the ESA Sentinels program, radar missions and high-resolution commercial systems.
- Includes extended coverage of radar and lidar processing methods.
- Covers new approaches to classification, including OBIA and machine-learning algorithms.
- Adds more focus on land surface characterization, time series, change detection, and ecosystem processes.

Praise for the Previous Edition

…a valuable book providing a thorough introduction into the field of earth observation … an ideal choice as a textbook for an introductory course on satellite remote sensing of the land surface. The text is well written and easy to follow, and as such highly recommended for students at the undergraduate level."
Dr. Jan G. P. W. Clevers, Wageningen University–*International Journal of Applied Earth Observation and Geoinformation, 2016*

"…a good textbook for teaching, a useful source for post-graduate researchers, and a valuable reference source for managers and practitioners."
Prof. John van Genderen – University of Twente –*International Journal of Digital Earth, 2016*

"… an extremely informative and useful resource for students, instructors, researchers, and professionals in the geospatial field and in ecology. Not only does the book discuss issues in a concise and clear way, but the graphics and imagery used are very informative and help to clarify potentially confusing concepts. The bibliography is particularly helpful as it allows the reader to easily delve into detail on a certain topic."
Dr. Lucia Lovison-Golob, – *WAML Information Bulletin, 2016*

"Chuvieco provides a complete overview of satellite remote sensing containing a suitable mix of theory and interesting practical examples … a valuable resource for environmental practitioners.
Luke Wallace, RMIT University –*Journal of Spatial Information Science, 2017*

All figures are available as PowerPoint presentation files. They can be downloaded from the CRC Press website:
http://www.crcpress.com/product/isbn/9781138583832

cover image courtesy of ESA/ATG medialab

Environmental Science

CRC Press
Taylor & Francis Group
an informa business
www.crcpress.com
CRC Press titles are available as eBook editions in a range of digital formats

ISBN 978-1-138-58383-2
9 781138 583832

Fundamentals of Satellite Remote Sensing
Third Edition
Chuvieco

Fundamentals of Satellite Remote Sensing

An Environmental Approach

Third Edition

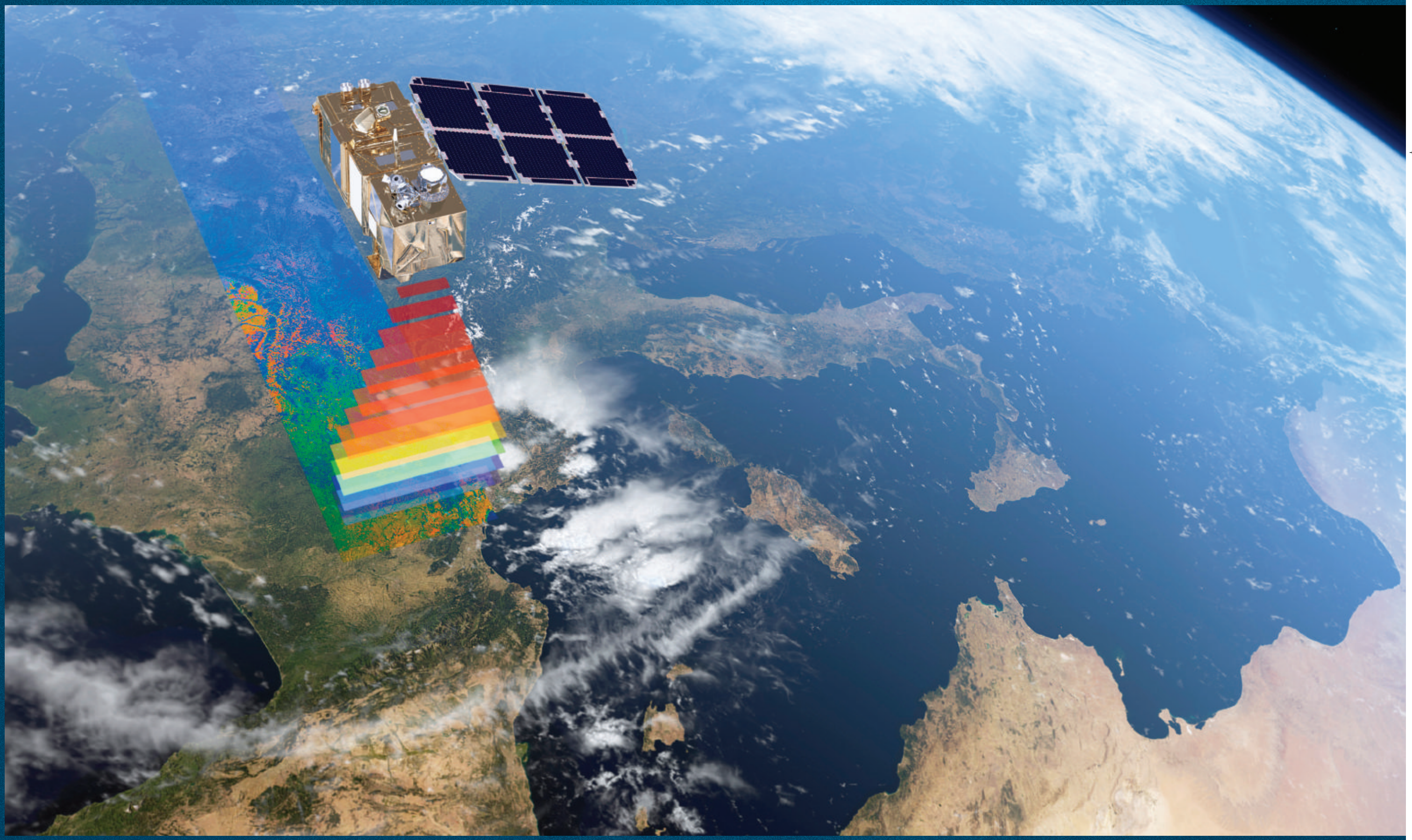

Emilio Chuvieco

CRC Press
Taylor & Francis Group

Fundamentals of Satellite Remote Sensing

Fundamentals of Satellite Remote Sensing

An Environmental Approach

Third Edition

Emilio Chuvieco

CRC Press
Taylor & Francis Group
Boca Raton London New York

CRC Press is an imprint of the
Taylor & Francis Group, an **informa** business

CRC Press
Taylor & Francis Group
6000 Broken Sound Parkway NW, Suite 300
Boca Raton, FL 33487-2742

Printed on acid-free paper

International Standard Book Number-13: 978-1-138-58383-2 (Hardback)

Visit the Taylor & Francis Web site at
http://www.taylorandfrancis.com

and the CRC Press Web site at
http://www.crcpress.com

To all mothers…

Because they chose to give us life

Contents

Preface

The growing concern about the present environmental problems and future sustainability of our planet has spurred great interest in monitoring the main variables of the Earth system. We need to gain a better understanding of the biogeochemical cycles to enhance our efforts to mitigate or adapt to future changes. The impacts of climate change, deforestation, desertification, fire, floods, and other natural and man-made disturbances require an updated, spatially comprehensive, and global source of geographical data. Human beings have demonstrated their capacity to dramatically alter Earth's natural systems with both beneficial and negative consequences.

Albert Einstein said that information is not knowledge, and certainly good information does not necessarily provide good knowledge, but the opposite is true, since bad information implies bad knowledge and most probably poor management. If we want to improve the way we manage our planet, to better appreciate its beauty and fragility, to make wiser decisions for the benefit of current and future human beings, to maintain essential ecosystem services, or to restore damaged landscapes, we definitely need accurate and updated information. Good decisions can only be based on good information.

Satellite Earth Observation (EO) is one of the most powerful tools to acquire accurate and updated information on the state of our planet. Data being collected by sensors on board EO satellites have revolutionized our knowledge of the planet's environment. They provide global, recurrent, and comprehensive views of the many dynamic processes that are affecting the resources, and habitability of our planet. Watching how our planet changes from space may not be sufficient to modify our current way of living, but it will certainly help us to manage our resources more wisely and move toward more sustainable practices.

This book is a modest attempt to help students and professionals become more familiar with the satellite EO technology. Many books have already been published on this topic, which I obviously do not try to amend. This text focuses on satellite observation systems and intends to provide an environmental orientation of the different interpretation techniques. EO includes a multitude of airborne or unmanned aerial vehicle (UAV) sensors (aerial photography, videography, light detection and ranging [lidar] and radio detection and ranging [radar][1] systems). These aerial platforms are particularly valuable in local studies, as well as in the validation of satellite data. However, this textbook will concentrate on satellite EO systems, as they provide worldwide coverage with an ample variation of spatial, spectral, and temporal detail, which make them suitable for a wide range of studies.

The second distinctive element of this textbook is the environmental approach. We target the text to scientists that are mostly interested in retrieving information from satellite data, rather than to those designing the sensors or the platforms. We hope the text will be useful for a wide range of environmental scientists, including geographers, biologists, geologists, ecologists, foresters, agronomists, pedologists, oceanographers, atmospheric scientists, and cartographers. We will mostly deal with terrestrial applications, but some examples of atmospheric and oceanographic uses of remote sensing data will be considered as well.

This book is organized in two sections. In the first part, we cover the basic processes that allow for the acquisition of space-borne imagery, including the physical principles of energy transmission and image acquisition; optical, thermal, and microwave radiant energy interactions on the Earth's surface (Chapter 2); and an overview of some of the main satellite observation systems (Chapter 3). The remaining chapters focus on visual and digital image analyses and interpretation techniques and their applications to science and management (Chapters 4 through 8). The final

[1] Following a well-accepted rule, throughout this book, acronyms will be written in lower case when they spell out a pronounceable syllable or syllables, and do not confuse with another word, as it is the case of lidar or radar.

chapter is devoted to the integration of remote sensing with geographic information system (GIS) for environmental analysis (Chapter 9). A basic knowledge of aerial photointerpretation is assumed, and the main effort here is dedicated to digital image analysis, which is amply covered in Chapters 6 and 7. However, Chapter 5 deals with visual analysis of satellite images, trying to offer a synergic use of visual and digital interpretation techniques. These three chapters are the nucleus of the book, dedicated to methods to extract information from satellite images. The first chapter is introductory. It presents an overview of remote sensing with discussion on its foreseeable developments and some remarks on legal issues and international debate concerning EO across national boundaries.

This book was initially published in Spanish in 1990 and was updated periodically in the same language. This edition is based on the second English version published in 2016. The first one was published in 2010 with the help of Professor Alfredo Huete. In addition to translating all the material, we tried to adapt the contents to a more international audience. The second edition updated contents of the previous one, including about 50% of new figures and changing the book style. This third edition adds or modifies about 15% of figures, includes new sections on radar preprocessing, alternative techniques for measuring vertical properties, new classification algorithms based on machine-learning approaches, new processing techniques sustained by cloud-computing services, and new validation approaches.

This edition maintains full color in all figures, so the reader can better appreciate the quality of information provided by EO satellite missions. Formulas are referenced using parentheses and are numbered sequentially, preceded by the number of the chapter, in the same way as the figures. We have illustrated the different interpretation techniques using a set of sample images acquired from different ecosystems and at different spatial resolutions. The purpose was to facilitate the reader the understanding of different methods by using the same study sites in each major section of the book.

All figures are available as PowerPoint presentation files. They can be downloaded from the CRC Press website: http://www.crcpress.com/product/isbn/9781138583832. I hope this addition will help students and professors to improve the educational content of the book.

I am grateful to the publishing company for their support in the process, particularly to Irma Britton and Rebecca Pringle, who have always being very responsive and attentive. I also need to acknowledge the valuable suggestions of colleagues and students who have helped me to correct errata from the previous editions and to shape the text in a more pedagogical way.

Writing a textbook is really a difficult task that is highly underappreciated by current academic evaluation criteria. My main interest in carrying out this job was to help students and colleagues discover a fascinating view or our beautiful planet, as observed from above the atmosphere, and to facilitate their learning of concepts and tools so that they can make a more effective use of satellite EO data for the benefit of humankind.

Emilio Chuvieco
Alcalá de Henares, Spain, August 2019.

Author

Emilio Chuvieco is a professor of geography and director of the Environmental Ethics Chair at the University of Alcalá, Spain, where he coordinates the Master program in Geographic Information Technologies. He also leads the "Environmental Remote Sensing Research Group." He was a visiting professor at the University of California at Berkeley and Santa Barbara, the Canadian Remote Sensing Center, Cambridge University, and the University of Maryland. He has taught postgraduate courses in 22 countries. He has been the advisor of 36 Ph.D. dissertations and the principal investigator of 33 research projects and 22 contracts. For the last nine years, he has been the science leader of the Fire Disturbance project within the European Space Agency's Climate Change Initiative Program. He is the author of 29 books and 370 scientific papers and book chapters. He has been a corresponding member of the Spanish Academy of Sciences since 2004, and he is the former president of the Spanish Remote Sensing Society. He is currently a co-editor in chief of the journal *Remote Sensing of Environment*.

1 Introduction

1.1 DEFINITION AND OBJECTIVES

One of the earliest dreams of humans has been to observe the Earth and its landscapes from a bird's perspective. This was only possible with the advent of balloons, gliders, and airplanes. A key driving force in our quest to fly above the ground has been to find new perspectives from which to observe the Earth's diverse landscapes. Our view of the Earth is quite limited when we are confined to the ground. Our desire to survey entire landscapes, mountain ranges, volcanoes, hurricanes, rivers, and ice fields has been evident since the beginning of aeronautics and now forms the foundation of space-based remote sensing or just EO. Today, as a result of rapid technological advances, we routinely survey our planet's surface from different platforms: low-altitude UAVs, airplanes, and satellites. The surveillance of the Earth's terrestrial landscapes, oceans, and ice sheets constitutes the main goal of remote sensing techniques. The term "remote sensing" was first coined in the early 1960s to describe any means of observing the Earth from afar, particularly as applied to aerial photography, the main sensor used at that time. In a broader context, remote sensing activities include a wide range of aspects, from the physical basis to obtain information from a distance, to the data acquisition, storage, and interpretation processes. Finally, the remotely collected data are converted to relevant information, which is provided to a vast variety of potential end users: scientists, farmers, fishers, consultants, journalists, land managers, etc. Nowadays, satellite images have become widely accessible by ordinary people, who use them within well-known images or map services, as a basis for planning tourist routes or finding shops and services.

Remote sensing (RS) may be more formally defined as the acquisition of information about the state and condition of an object through sensors that do not touch it. A remote observation requires some kind of energy interaction between the target and the sensor. The sensor-detected signal may be solar energy (from the Sun) that is reflected from the Earth's surface or it may be self-emitted energy from the surface itself. In both cases, the sensors collect energy coming from external sources and, for this reason, are called passive receivers. Other sensors produce their own energy pulses and therefore are able to observe the Earth's surface with their own observation conditions. The radiant energy signal that is detected and measured by the satellite sensor is then either stored in memory on board the satellite or transmitted to a ground receiving station for later interpretation. RS also includes the analysis and interpretation of the acquired data and imagery. Extracting relevant information requires a good understanding of the physical basis and the acquisition process, as well as a solid knowledge of the algorithms used to process the original data.

In summary, RS includes the following six components (Figure 1.1):

1. An energy source, which produces the electromagnetic radiation that interacts between the sensor and the surface. The most important source of energy is the Sun, as it illuminates and heats the Earth.
2. The Earth's surface, consisting of vegetation, soils, water, rocks, snow, ice, and human structures. These surfaces receive the incident energy from the source (1) and, as a result of physical and chemical interactions with the incoming energy, reflect and emit a part of that energy back toward the satellite sensor. Part or the whole energy pulse may be filtered by the atmosphere, depending on its gas and particulate matter concentrations.
3. Sensor and platform. The sensor is the instrument measuring and recording the energy coming from the surface. The platform provides the major services for sensor operation, such as attitude and orbit control, power supply, and communications with the ground

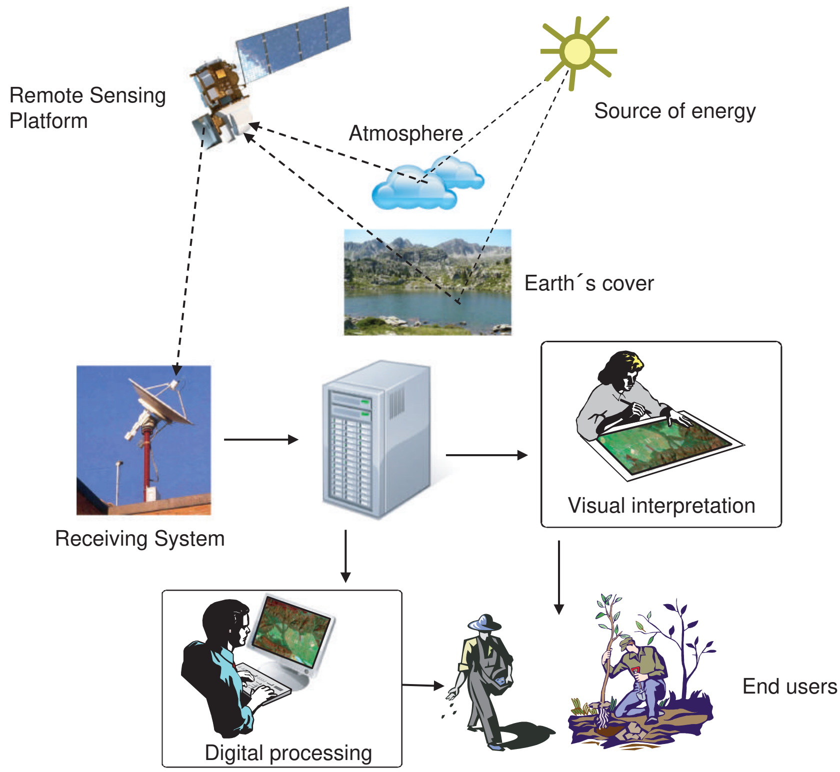

FIGURE 1.1 Illustration of the main components associated with RS activities.

receiving system. Ordinarily, an EO satellite includes different sensors, depending on its main mission. Meteorological satellites commonly include sensors to detect atmospheric humidity, temperature, albedo, ozone, or aerosol concentrations.

4. The ground receiving system collects the raw digital data measured by the sensor, stores the data, and formats them appropriately. Some basic preprocessing corrections are performed by the ground system, prior to the distribution of the imagery.
5. The analyst, who converts the processed image data into thematic information of interest, using visual and/or digital techniques.
6. The user community, which utilizes the information extracted from the data for a wide variety of applications.

We can illustrate the six components by using the human eye as an example. The eye is a sensor (3) that sees the reflected sunlight (1) from the various objects observed (2). The received electromagnetic signal is transmitted to the brain (4), which then generates an image of what is observed. The observer (5) further analyzes and interprets the image and, as the end user (6), applies this knowledge toward making appropriate decisions concerning his or her own behavior. Human vision is a sophisticated and complete RS system, providing great spatial and color detail.

Despite the sophisticated nature of human eyesight, our personal RS capabilities have several important limitations. Our eyes are restricted to a narrow portion of the electromagnetic spectrum, known as the "visible region." Other forms of electromagnetic energy, such as infrared, microwave, and ultraviolet radiation, cannot be seen with our eyes. In addition, our vision is dependent on a source of external energy, and we are unable to see if objects are not illuminated by the Sun or a source of artificial light. On the other hand, we have a limited perspective constrained by our own height, which restricts our observing capabilities to a limited, and often oblique, point of view.

RS techniques make it possible for us to overcome these limitations through the use of devices that provide information from nonvisible radiations, at different perspectives, and regardless of solar conditions.

These new capabilities have not only greatly expanded our knowledge about the Earth's environment but also provided increasing monitoring capabilities, to detect relevant changes. RS, in conjunction with parallel developments in GISs, global positioning systems (GPSs), and other ground data collection systems (field work, weather or hydrological stations, micro-sensors, etc.), now provides vast amounts of information about the land surface, to improve our understanding of the Earth system and better contribute to preserving it.

The effective utilization of such enormous quantities of data is accomplished with the growing availability of computer processors, which perform the tedious and time-consuming tasks of data handling and transformations to enable quick and efficient user interpretations and problem solving. Digital analysis of satellite data extends our capability to integrate spatial information, by combining information from different sources (soil or land cover maps, terrain models, climatic data, etc.). By enhancing our analytical capacity, we are able to focus more on data interpretation, problem solving, and making appropriate management decisions, tasks in which human intelligence is irreplaceable.

1.2 HISTORICAL BACKGROUND

RS, as an applied tool and methodology, has evolved historically in parallel with other technological advancements, such as the improvements in optics, sensor electronics, satellite platforms, transmission systems, and computer data processing. These developments have resulted in enormous progress in the quantity, quality, and diversity of data available to the scientific community (Beardsley et al. (2016). A summary of milestones in RS observation is included in Figure 1.2.

The first RS acquisition can be traced back to the mid-1800s, along with the development of aerial photography. In 1839, the first-ever photos were taken in France by Daguerre, Talbot, and Niepce, and by 1840, the French began using photos to produce topographic maps. In 1858, the first aerial photos were taken from a height of 80 m over Bievre, France, by Gaspard Félix Tournachon using cameras mounted on a hot-air balloon. The first balloon photographs used for urban planning were acquired by James Wallace Black in 1860 over the city of Boston. The first attempts to use the new perspective provided by aerial platforms in military reconnaissance occurred in 1861, during the American Civil War, when Thaddeus Lowe was appointed Chief of the Union Army Balloon Corps by President Abraham Lincoln. In the 1880s, the British used kites to obtain aerial photography, and in the early 1900s, carrier pigeons were able to fly as more advanced, smaller,

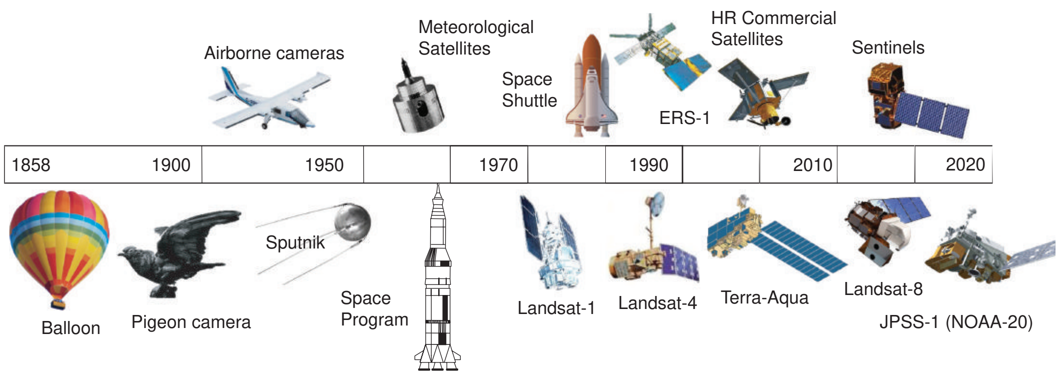

FIGURE 1.2 Historical development of RS systems.

and lighter cameras were developed. The great San Francisco earthquake of 1906 was captured on film using a panoramic camera mounted 600 m above San Francisco Bay and supported by a string of kites.

The next major milestone in RS occurred in 1909, when Wilbur Wright shot the first photographs over Italy from an airplane, establishing a new era of observations from airborne platforms. By 1915 and during World War I, the British Royal Air Force was collecting aerial reconnaissance photos with cameras designed specifically for aircraft surveying (Brookes 1975). In 1930, the first aerial multispectral photographs were collected by Krinov and colleagues in Russia. The following year, the first near-infrared film was developed and tested by Kodak Research Laboratories.

In the 1940s, the military made significant advancements in the development and use of color infrared films, which were used to distinguish real vegetation from camouflaged targets that were painted green to look like vegetation. The greatest developments in aerial reconnaissance and photo interpretation were made during World War II. Other significant advancements were made with thermal scanners and imaging radar systems, which create images by focused radar beams that scan across an area.

In the late 1940s and early 1950s, improved navigation systems gave way to the first space-based sensor devices. Early experiments with the V2, Aerobee, and Viking rockets recorded panoramic images of the SW United States from altitudes of 100–250 km. The first photo taken from space was acquired on March 7, 1947, at about 200 km above New Mexico while testing captured German V2 rockets (Figure 1.3). In 1950, scientist Otto Berg pieced together several photos from one of these tests into a mosaic of a large tropical storm over Brownsville, Texas.

One of the main strategic objectives of the Cold War era was the space race. The launch of Sputnik by the Soviet Union in 1957 was the start of a long series of civil and military missions that enabled us to explore not only our planet but also the Moon and neighboring planets. In April 1960, NASA launched the Television Infrared Observation Satellites (TIROS1) that began relaying continental views of global cloud patterns (Figure 1.4). These repetitive images enabled a deeper understanding of atmospheric conditions and circulation patterns, and provided early warnings of serious natural catastrophes.

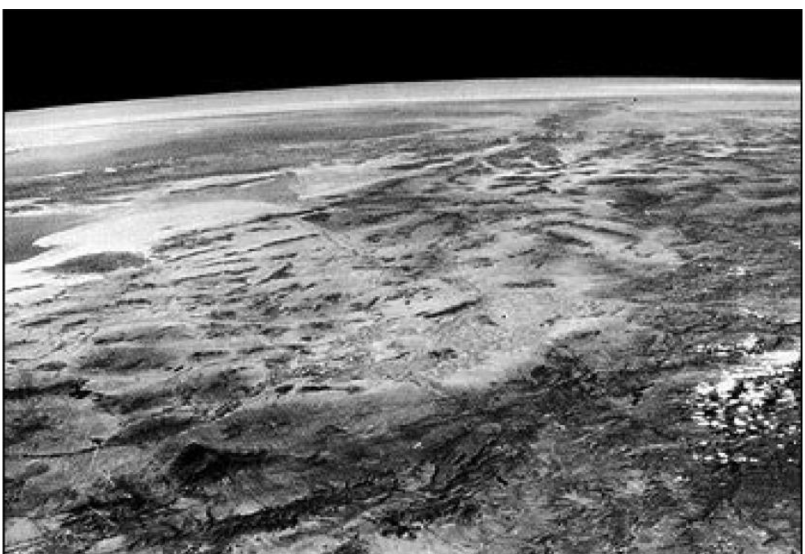

FIGURE 1.3 This photo was taken by an automatic K-12 camera, using black-and-white infrared film, from a Viking sounding rocket that reached a height of 227 km. This scene spans parts of New Mexico, Arizona, Nevada, California, and NW Mexico (upper Gulf of California on the left). (From the NASA archive.)

FIGURE 1.4 The TIROS was the first weather satellite, launched on April 1, 1960. (Source: https://www.flickr.com/photos/nasacommons)

In the 1960s, several manned missions were launched to explore our Solar System and to reach the Moon, but these missions also acquired valuable images of our planet. Astronauts provided us with breathtaking and scientifically useful images of the Earth during the Mercury and Apollo programs. The scientific value of exploring our planet from space became particularly evident in the last Mercury mission, in May 1963, in which NASA astronaut Gordon Cooper took a series of spectacular photographs with a hand-held Hasselblad camera over many regions inaccessible to Western scientists, such as the terrain of Central Tibet. These photographs provided valuable information about the geology, hydrology, and vegetation of remote regions and provided the impetus for the creation of space programs devoted to the study of the planet Earth.

The first mission that officially incorporated photography to investigate potential geological and meteorological applications of space technology was the Gemini Titan Mission in 1965. The Apollo 6 and Apollo 7 missions in 1968 also had strong photographic components (Figure 1.5), and in 1969, Apollo 9 carried the first multispectral EO package, which consisted of four Hasselblad cameras with different filters.

On December 24, 1968, Apollo 8 William Anders took an impressive picture of the Earth rise over the Moon. It was the first photograph of the Earth from another planetary body. This has been one of the most iconic photographs ever taken, portraying our planet as an isolated home, surrounded by the immense space (Figure 1.6).

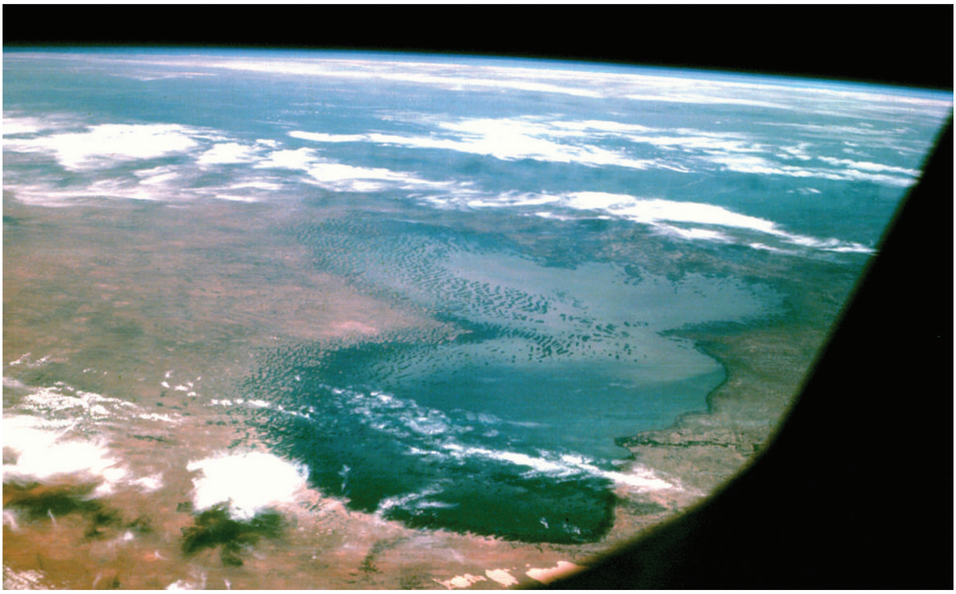

FIGURE 1.5 Photograph taken by the Apollo 7 over Lake Chad (Central Africa) in 1968. (From https://eol.jsc.nasa.gov/)

FIGURE 1.6 First ever photograph of our planet from another planetary body. It was taken in December 1968 by Apollo 8 crew. (From http://earthobservatory.nasa.gov/)

NASA, encouraged by the success of these early EOs, introduced digital technologies in RS in the late 1960s. Digital imaging sensors developed during the Ranger, Surveyor, and Lunar Orbiter probes provided key experience that aided the development of the first Earth Resources Technology Satellite (ERTS), launched on July 23, 1972. ERTS-1 was later renamed Landsat-1 with the launching of a second satellite in 1975, which provided the first detailed, high-resolution, multispectral images of the entire land surface of our planet.

The Landsat series continues today, providing a continuous and consistent high-quality 40+ year dataset of the Earth's land surface and its changes over time. This has been one of the most successful outcomes of EO, resulting in a wide range of civilian applications from the assessment of natural resources to the monitoring of natural disasters such as flooding, drought, fires, volcanic eruptions, and hurricanes. The Landsat missions were also accompanied by other NASA environmental observation projects, such as Skylab, a manned space laboratory in 1973; SeaSat, an oceanographic satellite in 1978; and the Heat Capacity Mapping Mission (HCMM) for thermal investigations in 1978.

As a result of the Landsat series's success, the decade of the 1980s saw an increasing interest by the international scientific community in developing space-borne EO systems. The most outstanding developments began with the launching of the first *Systeme Pour l'Observation de la Terre* (SPOT) satellite in early 1986 by the French *Centre National d'Etudes Spatiales* (CNES). The Japanese launched their first Marine Observation Satellite (MOS-1) in February 1987, while the Indian Remote Sensing (IRS-1) satellite was launched in March 1988. The European Space Agency launched in 1991 the first radar satellite, named the European Remote Sensing (ERS-1) satellite, followed by a second satellite with similar characteristics in 1995.

More recently, EO missions have increased exponentially, as will be discussed in more detail in Chapter 3. Benefiting from the experience and technical knowledge gained from the earlier launched missions, as well as the declining costs in the design of sensors and platforms, Russia, Canada, Germany, Italy, the United Kingdom, Brazil, Argentina, China, Spain, South Korea, Taiwan, and Israel, to mention some, have launched their own Earth-observing satellites for environmental and natural resource monitoring purposes. This trend has increased the worldwide availability and diversity of remotely sensed data while reducing acquisition costs for the end users.

Many of the civilian uses of RS have been the result of research performed for military applications. The delicate affair of the capture of a U-2 spy plane by the Soviets in 1960 led to the U.S. administration to make a great investment in developing military reconnaissance satellites, much less vulnerable than airplanes to detection and eventual bringing down. In 1995, some of the pictures taken by those military satellites were declassified, covering the period between 1960 and 1972, including high-resolution photos (from 2.5 to 7.5 m) from the Corona, Lanyard, and Gambit missions. In 2002 and 2011, other missions were declassified covering the KH-7 and KH-9 satellites with high-resolution photos acquired up to 1984. These photos are accessible through the long-term archive facility of the United States Geological Survey (USGS) Earth Resources Observation and Science (EROS) Center.

The private sector has also played an important role in promoting and advancing EO capabilities, through the creation of consortiums that have developed very high-spatial-resolution satellite projects. The first commercial satellites were launched in the late 1990s, the most famous being the IKONOS satellite launched by Space Imaging; the EROS A1, launched in 2000 by ImageSat International; and QuickBird, launched in October 2001 by DigitalGlobe. The role of the private commercial sector has greatly increased in the past decade, particularly related to applications requiring high spatial resolution, including homeland security and strategic observations, real state, tourism, location of services, commodities, and energy assets (Planet). This trend has extended traditional applications and users of satellite observation (Table 1.1). For instance, current satellite missions providing images with spatial resolutions in the range of 0.5–5 m are now acquired almost daily over the whole Earth using a constellation of small EO satellites. This information is very useful to monitor crop conditions, urban growing, and large public works, or to detect pipeline leakages. After natural or human disasters, these images are also particularly useful to provide a quick assessment to help urgent recovery actions (Figure 1.7) or monitor humanitarian activities, such as supervising conditions in refugee camps, or detect impacts of guerrillas in remote areas.

TABLE 1.1
Comparison of Traditional and New Users of RS Image Data

Traditional Users	New Users
Governments	News media information providers
Civil planners (mapping, land management, disaster response, etc.)	Electronic media organizations
	Print media
Armed forces	Trade journals
Intelligence services	
Scientific centers	
State and local governments	
Multinational Organizations	Non-government organization (NGOs)
UN agencies (e.g., UN Special Commission, UN High Commissioner Refugees)	Environmental policy
	Arms control, nonproliferation, and disarmament
Global change research programs	Regional conflict resolution
	Humanitarian relief
	Human rights
	Biodiversity, deforestation, etc.
Academia and research organizations	Academia and research organizations
Geography and geology departments	Media studies departments
Remote sensing programs	Security policy studies departments
Environmental studies	Archaeology departments
	Transportation studies
	Agricultural and ecosystem studies
Business	Business
Resource extraction (e.g., oil, gas)	Utilities (e.g., telecommunications, pipelines)
Resource management (e.g., forestry)	Insurance firms (e.g., hazard assessments)
	Precision agriculture
	Environmental impact assessments
	Energy companies
Remote sensing industry	Customers
Aerial photography firms	Real estate
Satellite imagery data providers	Individuals interested in images of their homes or cultural attractions
Value-added, image processing firms	
GIS firms	
Remote sensing professional organizations	

Source: Adapted from Baker (2001).

A recent report from Amnesty International in Nigeria on terrorist activities as detected by satellite images is particularly striking (Figure 1.8).

Recent trends point to a growing availability of satellite missions aiming to generate operational services, where remotely sensed data are routinely used. This is already the case of meteorological forecast where climate models are closely linked to diverse EO products (cloud temperature and height, moisture conditions, rainfall, wind fields, etc.). New EO missions include public access policies that facilitate an extended use of the acquired data. The quick Internet connections further facilitate the distribution of data, enabling the operation of near-real-time services. In addition to the raw and calibrated data, most of the recent programs include the development of corrected reflectances or temperatures and even second-order variables, thus facilitating the use of remotely sensed data even to nonexperts. The best example is the Moderate Resolution Imaging Spectroradiometer (MODIS) program, which has been able to derive 45 standard products from the raw data acquired by the Terra and Aqua NASA satellite (https://modis.gsfc.nasa.gov/, see Chapter 3). The Climate

FIGURE 1.7 GeoEye images acquired before and after the Japanese tsunami of 2011. The images were displayed by the New York Times web page. (From http://www.nytimes.com/)

Change Initiative of the European Space Agency (http://cci.esa.int/, last access June 2019) also offers a long-term data record or essential climatic variables, aiming to help modelers a better understanding of the climate system.

1.3 INTERNATIONAL SPACE LAW

Satellite RS systems collect images across the world without regard to political boundaries. This can lead to the violation of the national air space of a country and to the disclosure of its strategic information, which may be exploited by another country. Because of this, there has been much concern and discussion of the political, economic, and environmental consequences of space EO activities.

The first discussions on the legal aspects of aerial surveillance took place in the 1950s soon after the launch of the first spy satellites. At an international conference in Geneva in 1955, President Eisenhower proposed an Open Skies policy, which would allow free and mutual observations between the United States and the Soviet Union. The concept behind this failed proposal was to ease tensions and slow the arms race by allowing each nation to conduct aerial reconnaissance on the military resources of the other (Leghorn and Herken 2001).

FIGURE 1.8 Images acquired by Digital Globe satellites showing the impacts of guerrilla attacks on civilians in the north of Nigeria. (Acquired for Amnesty International. http://blog.amnestyusa.org/africa/the-story-behind-the-nigeria-satellite-images/)

The United Nations (UN) Committee on the Peaceful Uses of Outer Space (part of the UN Office for Outer Space Affairs, UNOOSA) is the primary international forum for the development of laws and principles governing outer space. One of its primary roles has been to develop basic legal principles on space observations to avoid tensions between observer and observed nations. Many developing countries have expressed the need to control the distribution of satellite images taken over their territory. Some countries, such as Brazil and Argentina, believe that the nation that owns a satellite system must first ask permission to remotely observe another country and that by no means should the data be handed over to third countries. In 1982, at the UN UNISPACE Congress in Vienna, an agreement was reached to facilitate the unrestricted access to imagery obtained over each nation and to require authorization from a country before disclosing imagery acquired within it to third countries (O.T.A. 1984). Russia and India proposed a 50 m spatial resolution limit of space-based observations to preserve sovereign military security, while the United States, the United Kingdom, and Japan were opposed to any restrictions whatsoever on data observation and distribution.

The UN sponsored the "Treaty on Principles Governing the Activities of States in the Exploration and Use of Outer Space, including the Moon and Other Celestial Bodies", also known as the Outer Space Treaty, which was adopted by the General Assembly and entered into force on October 10, 1967. Ninety-nine states have ratified, and an additional 26 have signed this treaty as of January 2008. The Outer Space Treaty provides the basic framework on international space law and guarantees that exploration and use of outer space shall be carried out for the benefit and in the interests of all countries. Additional principles governing the use of RS included in this treaty are as follows:

- Remote sensing shall promote the protection of the Earth's natural environment.
- Remote sensing shall promote the protection of humankind from natural disasters.
- The observed state shall have access to all primary and processed data acquired over its territory on a nondiscriminatory basis and on reasonable cost terms.
- The observed state shall also have access to the available analyzed information concerning the territory under its jurisdiction, taking particularly into account the needs and interests of the developing countries.
- States carrying out remote sensing activities shall promote international cooperation in these activities. To this end, they shall make available to other states opportunities for participation therein. Such participation shall be based in each case on equitable and mutually acceptable terms.
- Furthermore, a state must inform both the Secretary General of the UN, as well as the interested nations that request it, of the remote sensing programs that will be developed.

The growth and expansion of EO activities to many different countries and the increasing role of the commercial sector have lowered international concerns considerably. However, transferring space technology to developing countries has not been very effective, an unfortunate consequence considering that they are most in need of information about their natural resources. During the Third UN Conference (UNISPACE III) in Vienna in 1999, there were still concerns on the part of some countries (e.g., India and Israel) about the availability of RS data over their territories; however, the main concerns were in reducing the costs of satellite imagery and not in controlling data availability (Florini and Dehqanzada 2001).

The current treaty ruling international EO activities was signed in Helsinki, Finland, on March 24, 1992, and put in force on January 1, 2002, after being adopted by 26 nations (now 34). It is the most wide-ranging international effort to date to promote openness and transparency of military forces and activities. The treaty enables all participants, regardless of size, a direct role in gathering information about military forces and activities of concern to them. All Open Skies Treaty aircraft and sensors must pass specific certification procedures, and only treaty permitted sensors can be installed and launched. Open Skies aircraft may have video, optical panoramic, and framing cameras for daylight photography, infrared line scanners for day/night capability, and synthetic aperture radar for day/night all-weather capability. Collected imagery from Open Skies missions is made available to any participant state willing to pay the costs of reproduction. The treaty provides that at the request of any participant state, the observing state will provide it a copy of the data collected during a mission over the observed state.

At UN level, the international coordination of satellite EO is done through a dedicated committee (the Committee on Earth Observation Satellites, CEOS: http://www.ceos.org), which promotes exchange of data to optimize societal impacts of EO missions. Working groups within CEOS include one dedicated to quick assessment of natural hazards through a unified system of space data acquisition and delivery to countries affected by major disasters (International Charter on Space and Major Disasters). Other active groups are the calibration and validation, information system and services, and coordination of satellite constellations.

A recent resolution by the UN General Assembly encourages the use of EO data for supporting the international agreements related to the 2030 Agenda for Sustainable Development, the Sendai Framework for Disaster Risk Reduction 2015–2030, and the Climate Change Paris Agreement (United Nations 2018). This resolution acknowledges the importance of international cooperation and global partnership to continue developing the peaceful uses of outer space, by strengthening the long-term continuation of monitoring activities and the increasing exchange of technology and education among nations.

1.4 BENEFITS OF ENVIRONMENTAL MONITORING FROM SATELLITE SENSORS

Satellite EO has several advantages over other conventional methods of environmental sampling and monitoring, such as in situ field measurements or ground sensors. These methods are invaluable for calibration and validation purposes, but the temporal (for field methods) and spatial (for ground sensors) coverage is very limited. Therefore, they have a restricted use for spatio-temporal modeling of environmental phenomena. Satellite EO provides complementary benefits, which makes it a suitable information source for monitoring environmental changes at different spatial and temporal resolutions. The main potentials of this technique can be summarized in the following items.

1.4.1 Global Coverage

Satellite data are acquired by a platform that has a stable orbit around the Earth. Therefore, EO sensors make it possible to acquire consistent and repetitive imagery of the entire planet, including areas that are fairly remote and normally inaccessible, such as polar, mountain, desert, and forest areas. For example, EO has been found to be highly useful in mapping and monitoring ice sheets, a particularly relevant topic for water mass studies in the context of Arctic warming (Figure 1.9). Other examples include the use of RS in detecting remote forest fires or volcano eruptions, observing uncontrolled oil spills, and assessing damage from tsunamis or floods.

The global coverage provided by satellites is particularly useful in monitoring and understanding the dynamic processes affecting our environment. There is much concern over the many stresses placed on the environment, such as climate change, reduction in biologic diversity, depletion of freshwater, and land degradation and desertification. Tropical glaciers in the Peruvian Andes and the famous snows of Mount Kilimanjaro in East Africa are retreating rapidly and are predicted to disappear over the next two decades. By some estimates, as much as 40% of the Earth's land surface has been permanently transformed by human action, with significant consequences for biodiversity, nutrient cycling, soils, and climate.

Many of these environmental issues are most effectively addressed with a holistic planetary approach, for which global datasets, models, and information systems are needed. Assembling global databases is extremely difficult and time consuming and is often plagued by disparate data sources compiled with different criteria and formats. Country- or region-specific datasets must be merged and compiled to generate complete global datasets and images of the areas under study (Hengl et al. 2017). Satellite EO offers a quick and consistent source of uniformly collected data, from the same instrument and platform, with complete coverage of the planet for global studies.

The Global Climate Observing System (GCOS) program, part of the World Meteorological Organization (WMO), United Nations Educational, Scientific and Cultural Organization (UNESCO), International Council for Science (ICSU), and the UN Environmental Agency, has defined a set of 50 essential climate variables that can be retrieved and monitored by RS systems. They include atmospheric (over land, sea, and ice), oceanic, and terrestrial parameters. The most actively monitored are temperature, water vapor, precipitation, radiation budget, aerosols, greenhouse gases (Figure 1.10), ozone, sea level, sea ice, ocean color, snow cover, glaciers, ice sheets, albedo, land cover, fire disturbance, soil moisture, and leaf area index.

1.4.2 Synoptic View

Satellite sensors are located far from the Earth's surface, observing large areas and thus providing a synoptic view of landscape features. A standard 1:18,000 aerial photography covers an area of approximately 16 km^2. At a 1:30,000 scale, the area coverage increases up to 49 km^2. By comparison, a single Landsat operational line imager (OLI) image captures 31,000 km^2 and National Oceanic and Atmospheric Administration's (NOAA) Visible Infrared Imaging Radiometer Suite (VIIRS)

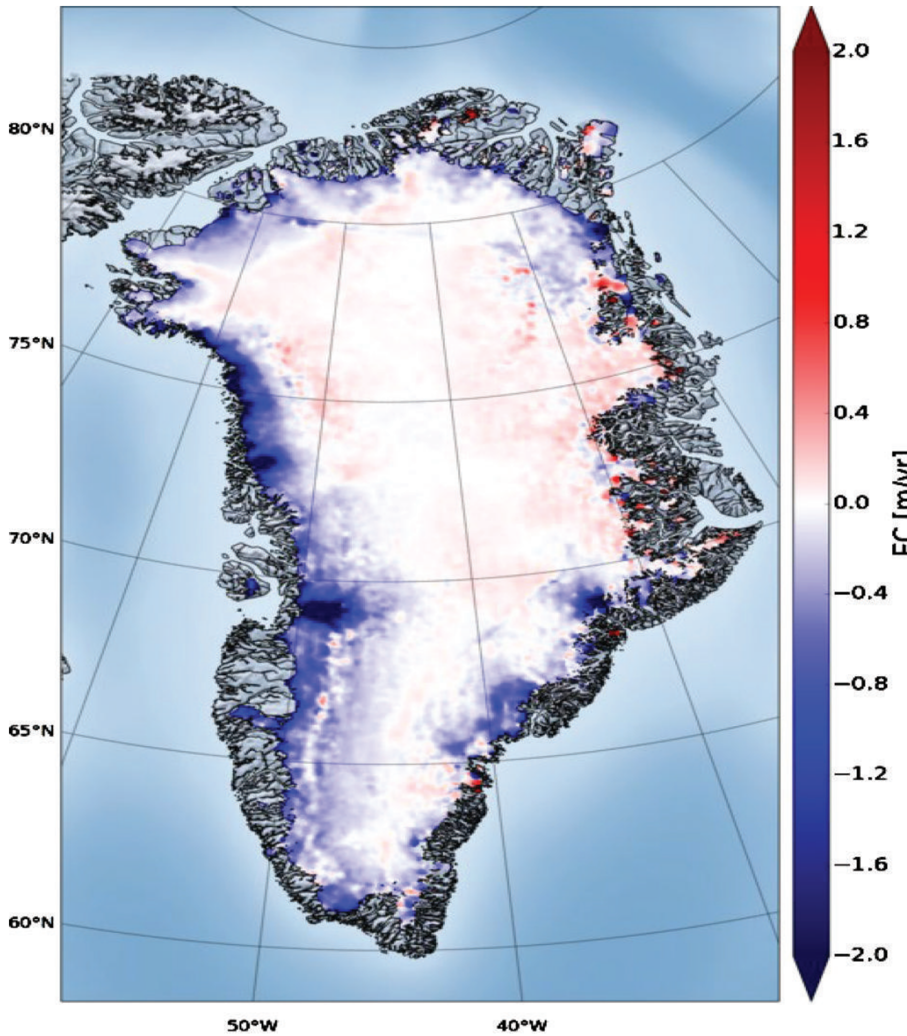

FIGURE 1.9 Greenland surface elevation change (EC) from Cryosat-2. Five-year means for 2011–2015 (http://products.esa-icesheets-cci.org/products/details/greenland_surface_elevation_change_cryosat2_v2.0.zip/).

image covers up to 9 million km^2. Satellite images are able to observe and depict phenomena that would be nearly impossible using the very local perspective of aerial photos. Large geologic features such as faults, fractures, and lithological contacts are more easily detected using satellite imagery, which can help locate mineral resources (Short and Blair 1986). It is also worth noting that satellite images cover such vast areas in a very short time, and therefore, the data are comparable throughout space, whereas conventional aerial photography requires mosaicking images acquired at different flight times.

1.4.3 Multiscale Observations

Satellite-based sensors, as will be discussed in more detail later, have a wide range of orbital altitudes, optics, and acquisition techniques. Consequently, the imagery acquired can be at very fine resolutions (fine level of detail) of 1 m or less with very narrow coverage swaths, or the images may have much larger swaths and cover entire continents at very coarse resolutions (>1 km) (Figure 1.11).

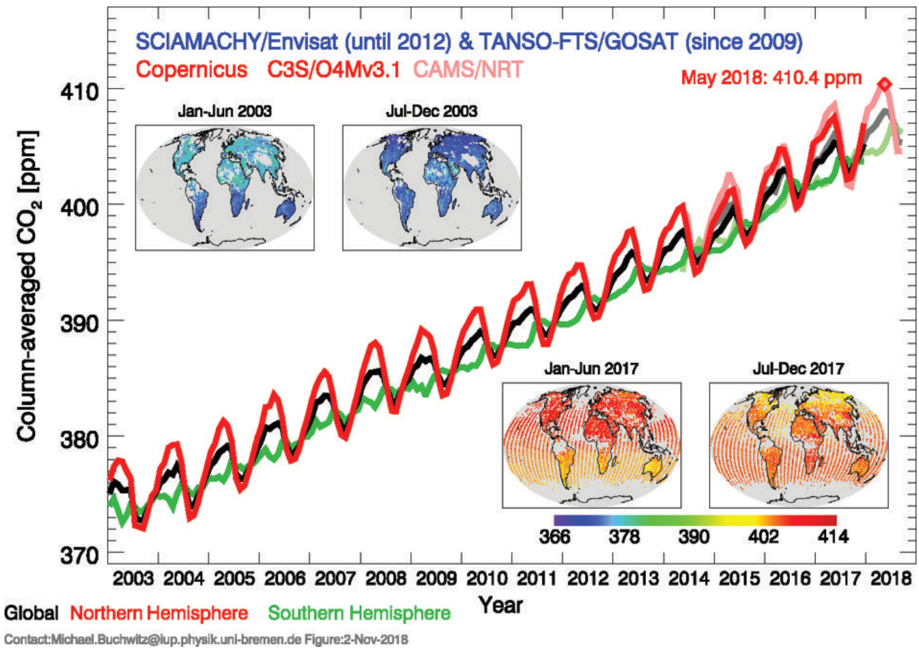

FIGURE 1.10 Atmospheric CO_2 time series as measured by the SCIAMACHY sensor on board the Envisat and Tanso-FTS on board the GOSAT. (Courtesy of Michael Buchwitz, University of Bremen: http://www.iup.uni-bremen.de/carbon_ghg/)

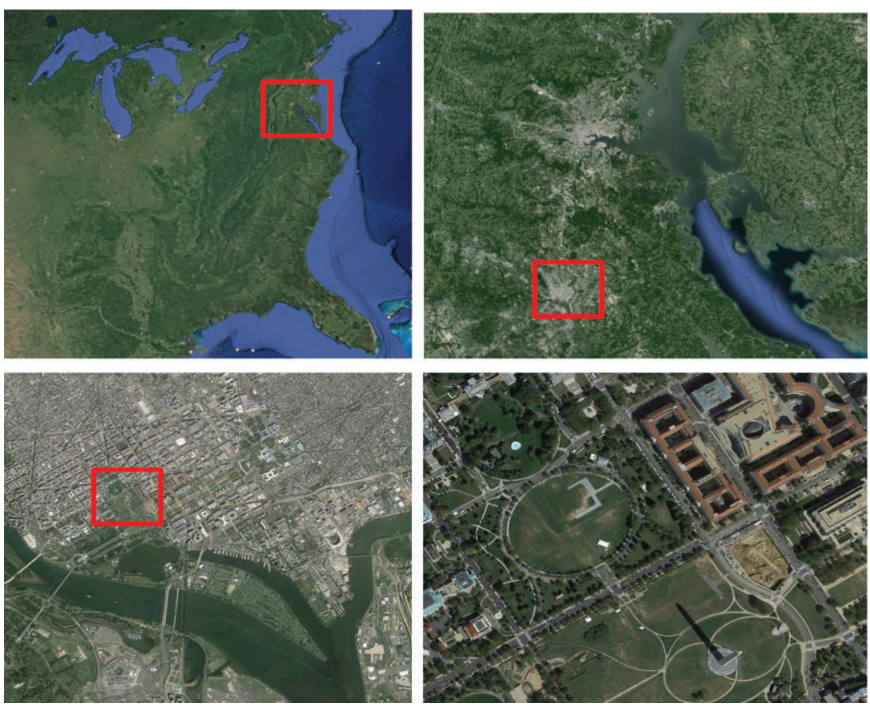

FIGURE 1.11 Satellite images from the U.S. East Coast acquired by different EO sensors. (Images extracted from Google Earth.)

The management and monitoring of the Earth's natural resources require spatial data at various scales, because the impacts of driving factors are often scale dependent (Ehleringer and Field 1993). For example, soil moisture may be more strongly related to local topography over short distances, and to regional precipitation patterns over longer distances. Remote sensing may be the only feasible means of providing spatially distributed data such as land use patterns, topography, and seasonal hydrologic and vegetation parameters at multiple scales and on consistent and timely bases.

1.4.4 Observations over the Nonvisible Regions of the Spectrum

Satellite sensors are capable of acquiring data over various portions of the electromagnetic spectrum that cannot be sensed by the human eye or conventional photography. The ultraviolet, near-infrared, shortwave infrared, thermal infrared, and microwave portions of the spectrum provide valuable information over critical environmental variables. For example, the thermal infrared portion of the spectrum allows us to study the spatial distribution of sea surface temperatures and marine currents, as well as water stress in crops. The ultraviolet radiation is critical to monitor the ozone layer. The middle infrared region is ideal to sense CO_2 concentrations, and the microwave radiation is more sensitive to estimate soil moisture and snow cover.

1.4.5 Repeat Observation

The orbital characteristics of most satellite sensors enable a repetitive coverage of the same area of the Earth's surface on a regular basis with a uniform method of observation. The repeat cycle of the various satellite sensor systems varies from 15 min to nearly a month. This characteristic makes RS ideal for multitemporal studies, from seasonal observations over an annual growing season to inter-annual observations depicting land surface changes (see Section 7.3). Such periodic observations are vital given the highly dynamic nature of many environmental phenomena. There are many examples of multitemporal applications of EO images, such as monitoring water bodies (Figure 1.12), drought and flooding patterns, snow cover melting, deforestation assessments, and meteorological phenomena.

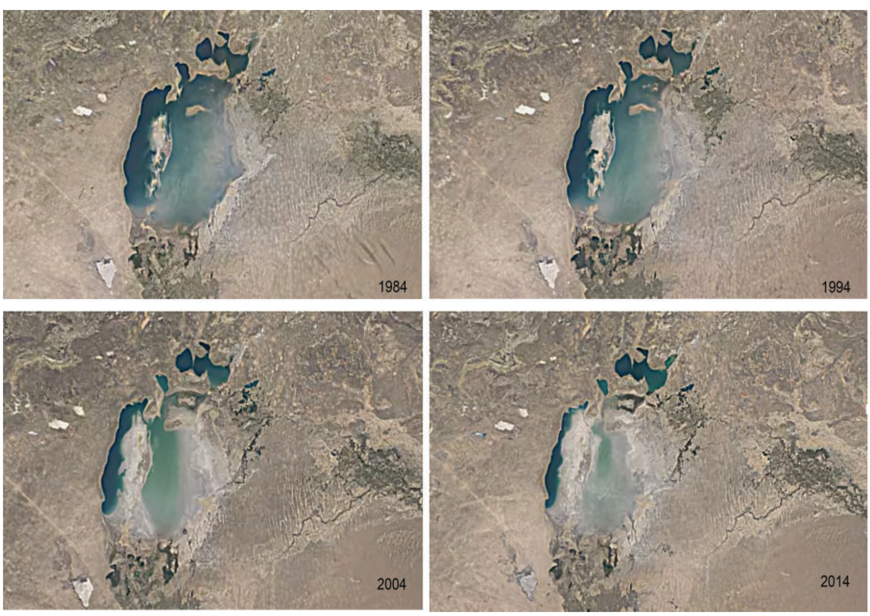

FIGURE 1.12 Multitemporal Landsat images acquired over the Aral Sea in Kazakhstan. (Images available at https://earthengine.google.com/timelapse/)

1.4.6 Immediate Transmission

Nowadays, all RS systems record image data in digital format, facilitating a real-time transmission to the ground receiving station and eventually to the end user. This is particularly relevant when dealing with disasters and natural hazards that require quick access to imagery (as it is the case of the International Disaster Charter).

Traditionally, only meteorological sensors had direct transmission to the end user, as the signal was not codified and could be acquired by a relatively cheap receiving antenna. Currently, images from global sensors can still be acquired freely, even from low-cost systems. In addition, the space agencies and commercial companies provide near-real-time data of images or even derived products. This is the case, for instance, of the information on active fires detected by the MODIS and VIIRS sensors that is sent by email to registered users within hours of satellite acquisition. For most medium- and high-spatial-resolution sensors, images can be obtained fairly quickly using fast Internet connections, but ordinarily not yet in real time as the signal is usually coded. These sensor systems transmit images when they are within the coverage area of the antenna or otherwise record on board for later transmission. The user obtains the image with a certain time delay, due to calibration and preprocessing of the data.

1.4.7 Digital Format

As most images are now in digital format, the integration of satellite-derived information with other sources of spatial data is relatively straightforward. Computer-assisted visualizations of image data are also possible, as in the generation of 3D views by combining satellite imagery with digital elevation models (Figure 1.13). These views can be created from different angles and under different simulated conditions.

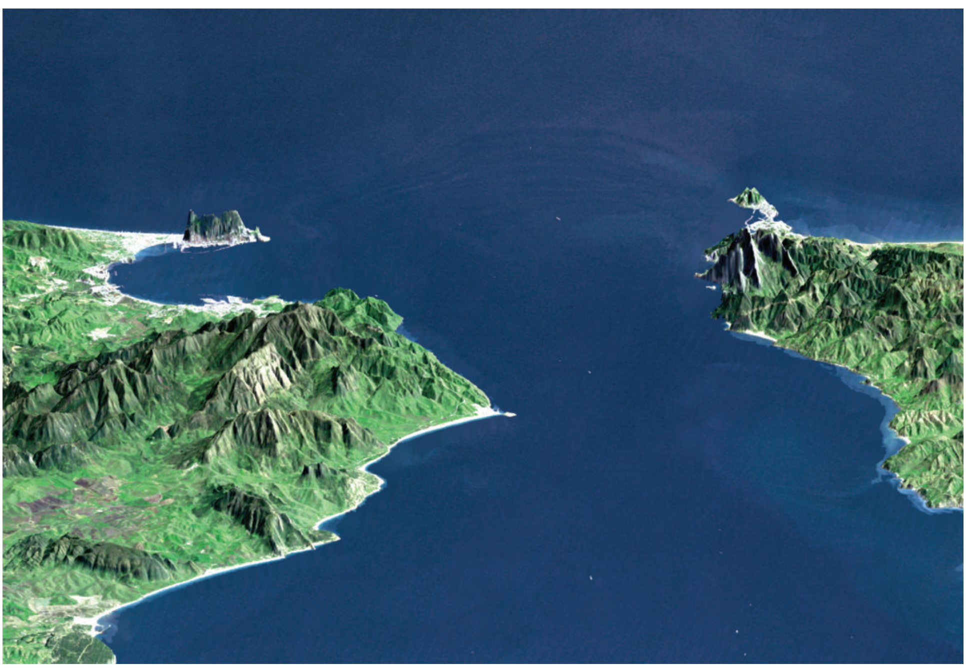

FIGURE 1.13 The Strait of Gibraltar in three dimensions, combining terrain data retrieved from the Shuttle Radar Topography Mission (see Chapter 3) with a pseudo-natural color image acquired by the Landsat Thematic Mapper (TM) in 1987. (From http://earthobservatory.nasa.gov/)

In summary, there are many advantages to the use of EO for the study and monitoring of the Earth's landscapes. However, this does not imply that EO satellites can be used to retrieve any environmental variable. Remote sensing also has limitations related to the available spatial, spectral, and temporal resolutions. The images may not be recorded at the required spatial detail or not frequent enough to cope with the user requirements. Furthermore, persistent cloud cover may notably reduce useful observations of optical sensors, thus severely restricting observations in cloudy areas. Radar observations are an alternative as they are independent of cloud coverage, but there are still few missions with radar capabilities and processing these data is more complex than for optical observations. On the other hand, current RS techniques may not be sensitive enough to detect the variable of interest. For instance, subsurface soil moisture or deep water temperature is unlikely sensed by EO systems, which receive radiation mostly from the upper layers of the surface.

In summary, EO satellite should be viewed as a complementary tool to other natural resource and environmental monitoring techniques, such as soil or plant samples, meteorological sensors, or flux towers, which in any case are useful to validate estimations provided by satellite instruments.

1.5 SOURCES OF INFORMATION ON RS DATA

Although RS science is only a few decades old, much has been written on this subject, including books, peer-reviewed papers, conferences, and technical reports. Some of the most important congresses are those organized by the professional societies dedicated to the development of RS. These organizations include the International Society for Photogrammetry and Remote Sensing (ISPRS), the Institute of Electrical and Electronics Engineers (IEEE) Geoscience and Remote Sensing Society (IGARS), the American Society of Photogrammetry and Remote Sensing (ASPRS), the Remote Sensing and Photogrammetry Society (RSPS), the International Society for Optical Engineering (SPIE), and the European Association of Remote Sensing Laboratories (EARSeL).

The main scientific journals dealing with EO studies ranked by the impact factor (of 2019) are the following: *Remote Sensing of Environment* (8.218), *ISPRS Journal of Photogrammetry and Remote Sensing* (6.942), *IEEE Transactions on Geoscience and Remote Sensing* (5.63), *International Journal of Applied Earth Observation and Geoinformation* (4.846), *Remote Sensing* (4.118), *International Journal of Digital Earth* (3.985), *GIScience and Remote Sensing* (3.588), *IEEE Geoscience and Remote Sensing Letters* (3.534), *IEEE Journal of Selected Topics in Applied Earth Observations and Remote Sensing* (3.392), *Canadian Journal of Remote Sensing* (2.553), *International Journal of Remote Sensing* (2.493), *Remote Sensing Letters* (2.024), *European Journal of Remote Sensing* (1.904), *Photogrammetric Engineering and Remote Sensing* (1.367), and *Journal of Applied Remote Sensing* (1.344). As it is known, the impact factor measures the relation between the number of citations and the number of papers published by a scientific journal in a certain period, and it is a common criterion to evaluate the relevance of a scientific publication.

There are a large number of textbooks dedicated to EO, spanning a range of orientations and scopes. These can be classified into two broad groups: those intended for a general audience and those written for specific application fields (hydrology, oceanography, land use, geology, etc.).

The first group of books can be further classified as follows: those that provide coverage of all the main topics of RS acquisition and interpretation, and those books that focus on specific topics, such as land cover classification, or the physical principles of image acquisition. The general textbooks group are the most common (Asrar 1989; Barret and Curtis 1999b; Campbell and Wyme 2011; Conway 1997; Couzy 1981; Cracknell and Hayes 1991; Curran 1985; Chen 1985; Danson and Plummer 1995; Drury 1998; Elachi 1987; Estes and Lenger 1974; Gibson and Power 2000a,b; Harper 1983; Harris 1987; Holz 1973; Hord 1986; Howard 1991; Jensen 1996, 2000; Lillesand and Kiefer 2000; Lira 1987; Liu and Mason 2016; Lo 1986; Maini and Agrawal 2014; Mather 1998; McCloy 1995; Quattrochi and Goodchild 1997; Rees 1999; Richards and Xia 1999; Robin 1998; Schanda 1976; Schowengerdt 2007; Short 1982; Slater 1980; Solimini 2018; Swain and Davis 1978; Szekielda 1988; Thomas et al. 1987a; Townshend 1981; Verbyla 1995; Weng 2012;

Wilkie and Finn 1996). Special category of general textbooks are those centered on specific sensors, such as radar (Allan 1983; Henderson and Lewis 1998; Lewis and Henderson 1999; Richards et al. 2010; Shimada 2018; Trevett 1986), or lidar systems (Beraldin et al. 2010; Dong and Chen 2017; Fujii and Fukuchi 2005; Vosselman and Maas 2010).

Another group of textbooks are those oriented toward specific applications: urban areas (Rashed and Jürgens 2010; Weng et al. 2018; Xian 2015), pedology and geology (Gupta 2017; Metternicht and Zinck 2008; Mulders 1987; Prost 2013; Rencz and Ryerson 1999; Short and Blair 1986), hydrology (Gower 1994; Hall and Martinec 1985; Robinson 1985), oceanography (Gower 1994; Martin 2014; Stammer and Cazenave 2017; Tang et al. 2011), climatology (Barret 1974; Carleton 1991; Conway 1997; Cracknell 2001; Islam et al. 2017; McConnell and Weidman 2009), natural vegetation (Achard and Hansen 2012; Franklin 2001; Frohn 1998; Hobbs and Mooney 1990; Howard 1991), forest fires (Ahern et al. 2001; Chuvieco 2003; Chuvieco 2009), archeology (Goodman and Piro 2013; Lasaponara and Masini 2012; Parcak 2009), and global change studies (Chuvieco 2008; Chuvieco et al. 2010; Purkis and Klemas 2011).

Access to satellite images is becoming easier, largely due to wide distribution through the Internet. For images acquired by NASA or other American programs, the USGS EarthExplorer (https://earthexplorer.usgs.gov/) and GloVis (http://glovis.usgs.gov/) (Figure 1.14) servers are the most accessible portals to download EO images. Many other space agencies and companies also provide free data, including the European Space Agency (ESA) and the Japanese Space Agency, JAXA. Commercial image services are also available through Google Earth, Telespazio, Airbus, and Planet, among others.

Many organizations provide free, downloadable versions of images in standard formats. Web searches provide the best guide, as the number and location of sites are evolving rapidly. At the time of writing this chapter (April 2019), the most interesting references for accessing visual satellite data are NASA Visible Earth (http://visibleearth.nasa.gov/), which includes sample images from all NASA missions, and the Google Earth Engine database (https://earthengine.google.org/#intro), which includes a full Landsat historical archive to observe changes in the Earth landscapes for

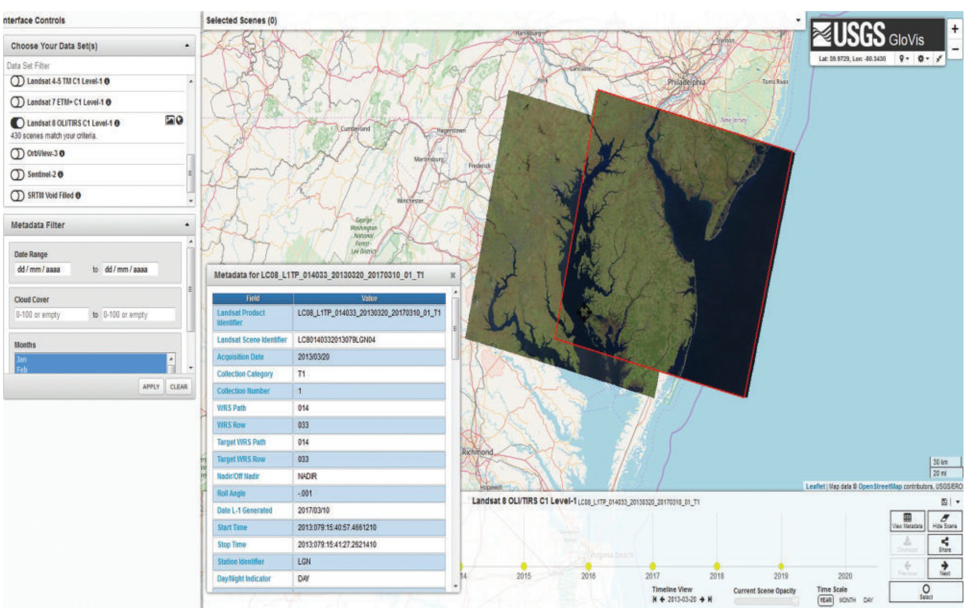

FIGURE 1.14 Visualization tool of the USGS to download images from different EO sensor systems. The screen shows an example of Landsat-8 images and metadata from the Eastern coast of the United States (http://glovis.usgs.gov/).

the last 35 years. The Copernicus Sentinel Hub of the ESA (https://scihub.copernicus.eu/) provides free access to data acquired by the different Sentinel missions, which included more than 220.000 registered users in April 2019.

Several books have been published in the last two decades compiling satellite images of different terrestrial landscapes. They provide an interesting source of information on the potentials of EO data, as well as a historical reference for analyzing land changes. Among the most relevant works are Mission to Earth (NASA 1976), Earthwatch (Sheffield 1981), Man on Earth (Sheffield 1983), Images of Earth (Francis and Jones 1984), Looking at Earth (Strain and Engle 1993), and the Satellite Atlas of the World (National Geographic 1999). Some may be now outdated.

1.6 REVIEW QUESTIONS

1. Identify a component that is not required for a RS system:
   a. Source of energy
   b. Image processing equipment
   c. Platform
   d. Sensor
2. Which of these properties favors satellite versus airborne RS?
   a. Spatial resolution
   b. Cost
   c. Temporal resolution
   d. Stereoscopic view
3. Which of these properties favors airborne over satellite RS?
   a. Spatial resolution
   b. Spectral resolution
   c. Temporal resolution
   d. Stereoscopic view
4. Which of the following satellite programs is managed by a private company?
   a. Landsat
   b. Planet
   c. NOAA
   d. Sentinel
5. Which of the following benefits of satellite EO is more beneficial for real-time monitoring?
   a. Direct transmission
   b. Digital format
   c. Global coverage
   d. Synoptic view

2 Physical Principles of Remote Sensing

2.1 FUNDAMENTALS OF REMOTE SENSING SIGNALS

Remote sensing means that something is sensed remotely, that is, from a certain distance. This implies that there is a certain interaction between the object and the sensor detecting it. For example, our eyes are sensors that can see a tree as they receive the visible (VIS) radiant energy reflected by that tree. But the tree needs to be illuminated by the Sun or other external energy sources. Our eyes would not be able to see the tree in total darkness. Still the tree is there, and we could detect it if we were able to detect the thermal energy that the tree radiates. Both reflected and emitted energy from the tree are closely linked to its chemical, biological, and physical properties, for instance, the number and position of its branches and leaves, or their pigment and water content. These components impact different types of electromagnetic (EM) energy. For instance, the pigment status of leaves affects the blue and red regions of the VIS spectrum, while water content has more impacts on the shortwave infrared (SWIR) and thermal infrared (TIR) bands. Similarly, reflected or emitted radiation from the Earth's surface provides critical information on the properties of soils, ice, snow, water, vegetation, and rocks. The goal of remote sensing is to understand how EM energy interacts with the surface so that we may better extract relevant information from the images (Solimini, 2018).

When we observe a tree, our eyes are sensitive only to the light the tree reflects. We can also use artificial sensors that are able to detect other sources of energy, for instance, thermal cameras that detect plant temperature. We could also use sensors with their own source of energy, such as laser or microwave (MW) pulses, which *illuminate* the tree and detect the return energy afterward. Thus, in remote sensing, we may consider three ways of sensing information about an object: by reflection, by emission, and by combined emission–reflection (Figure 2.1).

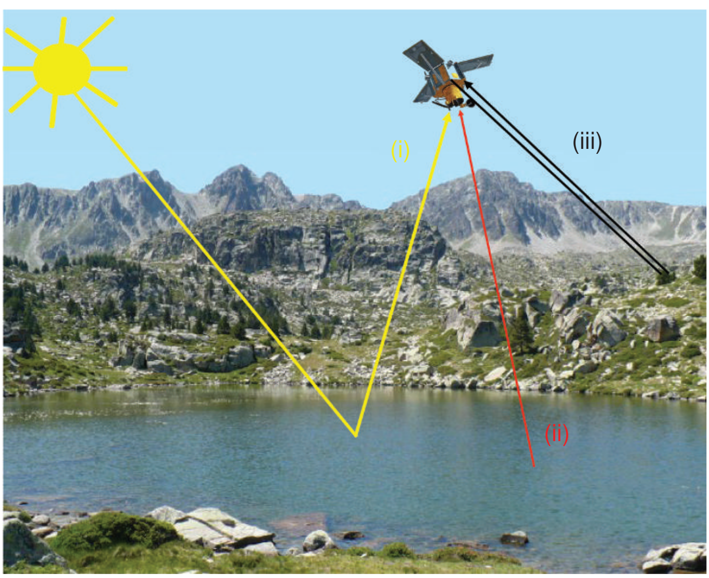

FIGURE 2.1 Main types of radiation processes in remote sensing: (i) reflection, (ii) emission, and (iii) emission–reflection.

The first one is the most common because it utilizes sunlight, the main source of energy on the Earth. The Sun illuminates the surface, which in turn reflects a portion of this energy back to space depending on the type and composition of cover present on the surface. The reflected EM energy is detected by the satellite sensor, which then records and transmits this signal to a receiving station.

Remote sensing observations may also be based on the emitted energy from the Earth's surface (Figure 2.1, ii), wherein the sensor detects energy coming from the surface itself. Since it does not directly depend on the Sun, this observation can be performed during both day and night. All objects warmer than absolute zero (0 K) emit energy, and the hotter the object, the higher the radiant energy it produces. The Sun is the hottest object, and it emits very large amounts of energy. Warm objects (a fire, lava, hot water) emit energy at longer wavelengths that we can sense with our skin, but not with our eyes.

Finally, we can also base remote sensing observations on active sensors, so named as they have their own source of energy. They are able to send pulses to the target objects and record later their reflection to characterize those objects. The most common active technique in the early days of remote sensing was radar, working with MW energy, but in the last decades, lidar sensors have also become very popular. They work with polarized VIS or near-infrared (NIR) light and are extensively used these days to measure distances.

We will review how these different sensors work in the next chapter. This chapter focuses on how the signal is generated and interacts with atmospheric components and surface covers in its way down to the Earth and reflected/emitted up to the sensor.

The properties of EM radiation may be explained by two seemingly contradictory theories of light: wave theory (Huygens, Maxwell) and quantum theory (Planck, Einstein). According to wave theory, EM radiation is a form of energy derived from oscillating magnetic and electrostatic fields that are mutually orthogonal to each other and to the direction of propagation (Figure 2.2). EM energy is transmitted from one place to another following a harmonic and continuous model with a constant velocity, $c = 3 \times 10^8\,\text{m s}^{-1}$ (speed of light). The properties of this energy can be described according to its wavelength (λ) and frequency (ν), which are related by

$$c = \lambda \nu \tag{2.1}$$

where λ is the wavelength or distance between two successive peaks (usually in micrometers, $1\,\mu\text{m} = 10^{-6}\,\text{m}$; or nanometers, $1\,\text{nm} = 10^{-9}\,\text{m}$), and ν is the frequency, or the number of cycles that pass over a fixed point per unit of time (in hertz, cycles s^{-1}).

As Equation 2.1 shows, the frequency of light is inversely proportional to its wavelength, such that the greater the wavelength, the smaller the frequency, and vice versa.

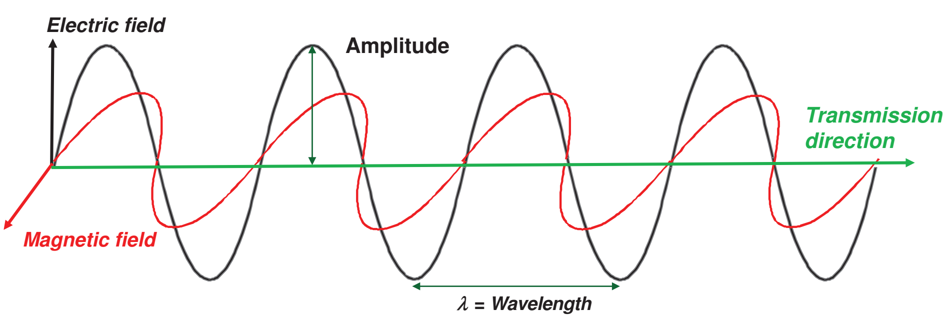

FIGURE 2.2 The oscillating electric and magnetic components of EM radiation propagation (the wave theory of light).

The quantum theory of light describes radiation as a succession of discrete packs of energy known as photons or quanta, with mass equal to zero. The amount of energy transported by a photon is proportional to its frequency:

$$Q = h\,\nu \tag{2.2}$$

where Q is the radiant energy of a photon (in joules, J), ν is the frequency, and h is Planck's constant (6.626×10^{-34} J s). Combining this with Equation 2.1 results in

$$Q = h(c/\lambda) \tag{2.3}$$

which implies that the greater the wavelength, or the smaller the frequency, the lower the energy content of an EM flow, and vice versa. This implies that it is more difficult to detect longer than shortwave energy radiations, as the former have lower energy and require more sensitive means of detection.

2.2 THE ELECTROMAGNETIC SPECTRUM

Since radiation sources are very diverse and therefore, EM radiations vary from very small to very long wavelengths, most textbooks tend to classify them in certain groups of wavelengths of frequencies that are finally organized in the so-called EM spectrum (Figure 2.3). It includes a continuous range of wavelengths or frequencies, but commonly several spectral regions or bands are identified, with particular radiation properties. Although most spectral bands are referred to in length units, MWs are commonly expressed in frequency units (gigahertz, GHz = 10^9 Hz).

The shortest wavelengths, with the highest radiation energy, are gamma rays and X-rays, whose wavelengths range from 10^{-9} to 10^{-3} µm (or 10^{-15} to 10^{-9} m) and which are commonly used in astronomical observation and medical applications, respectively. The longest wavelengths are used for telecommunications, radio, and television, with wavelengths in the range of 10^8–10^{10} µm (or 100–10,000 m).

The spectral regions most commonly used in remote sensing observation are the following:

1. The VIS region (0.4–0.7 µm). It covers the spectral wavelengths that our eyes are capable of sensing and at which the Sun's energy is the highest. The VIS region can be further divided into the three primary colors: blue (0.4–0.5 µm), green (0.5–0.6 µm), and red (0.6–0.7 µm) (Figure 2.3).
2. The NIR region (0.7–1.2 µm). This portion of the spectrum lies just beyond the human eye's perception capability. It is also known as the reflective infrared and in the past as photographic infrared because part of this spectral region (0.7–0.9 µm) could be detected with special films. The NIR is of special interest because of its sensitivity to determine plant health status.
3. The mid-infrared region (MIR, 1.2–8 µm). This spectral region lies between the NIR and TIR regions. From 1.2 to 2.5 µm, the influence of the Sun's energy is still very relevant, and this band is commonly referred to as the SWIR region, which provides the best estimations of the moisture content (MC) of soils and vegetation. From 2.5 to 8 µm, the signal becomes a continuous mixture of solar-reflected and a surface-emitted energy, becoming the more relevant the latter as the wavelengths increase. The 3–5 µm interval is particularly useful for detecting high-temperature sources, such as volcanoes or active fires.
4. The TIR region (from 8 to 14 µm). This is the emitted energy from the Earth's surface at normal ground temperature. The thermal region is widely used in detecting vegetation evapotranspiration (ET), ice and cloud thermal properties, or urban heat effects.
5. The MW region covers radiations longer than 1 cm. At these wavelengths, atmospheric absorption is low, which enables us to "see" through clouds. MW radiation can also

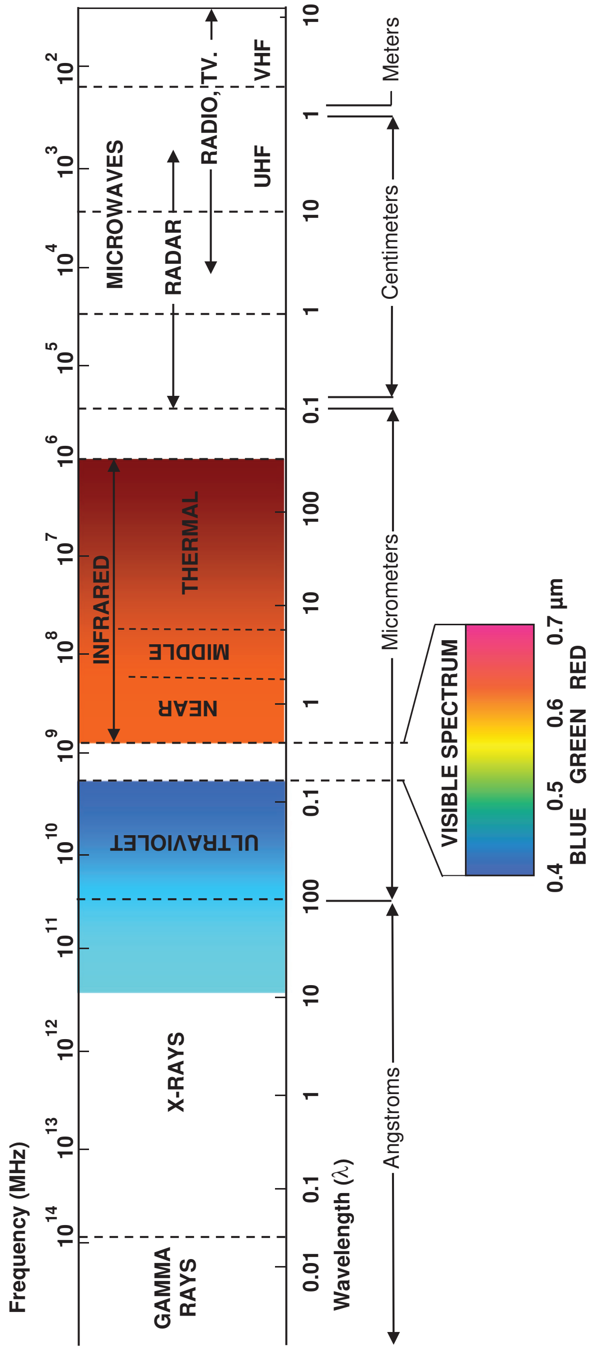

FIGURE 2.3 Major spectral bands within the EM spectrum.

penetrate forest canopies to various depths and is very useful in soil moisture and surface roughness analyses. It is mostly used by active sensors (radar), but there are also passive MW radiometers that have been used for soil moisture and ice monitoring.

The EM energy signals received by a sensor across these different spectral regions vary with the biophysical and biochemical properties of the different surface components. In addition, they are affected by different atmospheric components (water vapor, trace gases, and aerosols). In the following sections, we examine how the various components of the terrestrial surface behave over these spectral regions. However, first, we introduce some of the basic energy concepts and units of measurement used in remote sensing in order to gain a better understanding of the characteristic properties of space-borne measurements.

2.3 TERMS AND UNITS OF MEASUREMENT

As mentioned earlier, a remote observation requires an energy source and a sensor that can detect the EM energy leaving the Earth's surface toward the field of view of the sensor. The EM energy of interest has a certain intensity, spectral composition, and direction (i.e., the energy may be directed toward or away from the surface). Here, we describe the units commonly used in remote sensing applications. The precise formulas for each of these energy terms are included in Table 2.1 (Curran 1985; Elachi 1987; Rees 1999; Slater 1980):

1. Radiant energy (Q), measured in joules (J), is the most basic energy unit and refers to the total energy radiated in all directions away or toward a surface.
2. Radiant flux (ϕ), measured in watts (W), is the number of joules per second (J s^{-1} = W) and represents the rate of energy transfer in all directions per unit of time.

TABLE 2.1
Radiometric Quantities Commonly Used in Remote Sensing

Concept	Symbol	Equation	Measured Unit
Radiant energy	Q	—	joules (J)
Radiant flux	ϕ	$\delta\phi/\delta t$	watts (W)
Exitance	M	$\delta\phi/\delta A$	W m^{-2}
Irradiance	E	$\delta\phi/\delta A$	W m^{-2}
Radiant intensity	I	$\delta\phi/\delta\Omega$	W sr^{-1}
Radiance	L	$\delta I/\delta A{\cdot}\cos\theta$	W m^{-2} sr^{-1}
Spectral radiance	L_λ	$\delta L/\delta_\lambda$	W m^{-2} sr^{-1} μm^{-1}
Emissivity	ε	M/M_n	unitless
Reflectance	ρ	ϕ_r/ϕ_i	unitless
Absorptance	α	ϕ_a/ϕ_i	unitless
Transmittance	τ	ϕ_t/ϕ_i	unitless

sr, steradian, measure of the solid angle
μm, micrometer or micron (10^{-6}m)
M_n, exitance of a blackbody at the same temperature
ϕ_i, incident flux
ϕ_r, reflected flux
ϕ_a, absorbed flux
ϕ_t, transmitted flux
θ, angle formed by the energy flux direction and the normal.

3. Radiant flux density is the rate of energy transfer per unit area, measured in watts per square meter ($W\ m^{-2}$).
4. Radiant exitance or emittance (M) is the radiant flux density *leaving the surface* in all directions per unit area and per unit time ($W\ m^{-2}$).
5. Radiant irradiance (E) is the radiant flux density *incident upon* the surface per unit area and per unit time ($W\ m^{-2}$). It is the same concept as the radiant exitance, but in this case, it refers to the energy arriving at the surface rather than leaving the surface. For instance, we use *solar emittance* to refer to the energy leaving the Sun, and use *solar irradiance* to refer to the solar energy arriving at the Earth's atmosphere.
6. Radiant intensity (I) is the total energy leaving the surface per unit time and within a unit solid angle (Ω). The solid angle is a 3D angle that refers to the area of transmitted energy that a surface subtends and is measured in steradians (Figure 2.4). Radiant intensity is thus measured in watts per steradian ($W\ sr^{-1}$).
7. Radiance (L) is the total energy exiting in a certain direction per unit area and solid angle of measurement. It is the most fundamental term in remote sensing since it describes exactly what the sensor measures. Radiance is expressed in watts per square meter per steradian ($W\ m^{-2}\ sr^{-1}$).

   The foregoing energy terms may also be expressed in terms of wavelength basis and have the prefix *spectral* applied to them, such as spectral radiance or spectral irradiance. For example, the term *spectral radiance*, L_λ, refers to the energy output from a unit area, unit solid angle, and unit wavelength, or $L_\lambda = W\ m^{-2}\ sr^{-1}\ \lambda^{-1}$.

   There is also a series of dimensionless energy terms, varying from 0 to 1, that are widely used in characterizing the spectral properties of the Earth's surface.
8. Emissivity (ε): This is the relationship between the radiant exitance of a surface (M) and that of a perfect emitter at the same temperature (M_n). A perfect emitter is also known as a blackbody and has an emissivity of 1. Natural materials, on the other hand, are imperfect emitters with emissivity values ranging from 0 to <1. Emissivity values over different wavelengths are useful in characterizing materials.
9. Reflectance (ρ): This is the relationship between the energy reflected by a surface and the energy incident upon that surface.
10. Absorptance (α): This is the relationship between the energy absorbed by the surface and the energy incident upon that surface.
11. Transmittance (τ): This is the relationship between the energy transmitted through a surface and the energy incident upon that surface.

These unitless terms can also have spectral added to them, as in spectral reflectance. There are a few useful relationships that are derived from the aforementioned energy terms. The term "albedo"

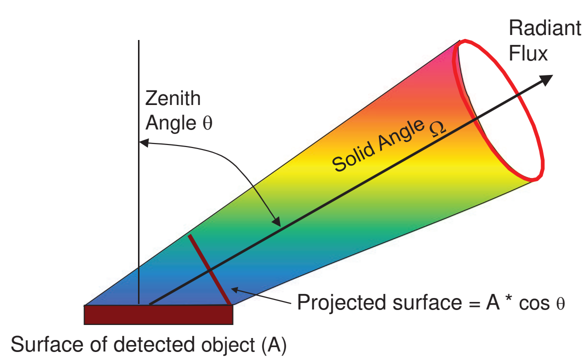

FIGURE 2.4 Solid angle and radiant energy changes with zenith angle.

is the ratio of all outgoing energy to the incident energy for a given surface area. More specifically, albedo is the ratio of exitance (M) to irradiance (E) over all solar reflective, or shortwave, wavelengths and is the equivalent of hemispherical reflectance, that is, the reflectance integrated over all directions (Equation 2.4). Albedo is a fundamental variable in energy balance studies, climate modeling, and soil degradation studies. Spectral albedo refers to the exitance divided by the irradiance for a specific spectral band (Equation 2.5):

$$\text{Albedo} = \rho_{\text{hemispherical}} = M/E \tag{2.4}$$

$$\text{Spectral albedo} = \rho_{\text{hemispherical},\lambda} = M_\lambda / E_\lambda , \tag{2.5}$$

It is important to note that a satellite sensor does not measure outgoing, hemispherical energy over all directions, but instead measures the directional radiance (L_λ) from only over a narrow angular field of view (Figure 2.4). The spectral directional radiance (L_λ) is related to the hemispherical spectral exitance (M_λ) as follows (Slater 1980):

$$M_\lambda = \pi L_\lambda \tag{2.6}$$

Similarly, the surface reflectances derived from satellite measurements are directional reflectances, as they refer to a specific measurement geometry between the satellite sensor and the Sun, relative to the surface. The relationship between the spectral radiance values received by a satellite sensor (L_{sen}) and the surface spectral reflectance (ρ_λ) becomes

$$\rho_\lambda = \pi L_\lambda / E_{0,\lambda} \tag{2.7}$$

where $E_{0,\lambda}$ is the solar irradiance arriving at the surface. We will further comment in Section 6.8.2 the impact of varying the observation geometry on the retrieval of ground reflectance.

2.4 ELECTROMAGNETIC RADIATION LAWS

There is a set of physical laws that govern the behavior and characteristics of EM radiation. We saw in Equation 2.3 that the energy content of EM radiation varies inversely with wavelength. The spectral distribution of EM radiation emitted by a blackbody (a perfect emitter) can be characterized by Planck's radiation law as follows:

$$M_{n,\lambda} = \frac{c_1}{\lambda^5 \left(e^{(c_2/\lambda T)} - 1 \right)} \tag{2.8}$$

where $M_{n,\lambda}$ (W m^{-2} µm^{-1}) indicates the radiant spectral exitance at a certain wavelength (λ in µm), c_1 and c_2 are the constants ($c_1 = 3.741 \times 10^8$ W m^{-2} µm^4 and $c_2 = 1.438 \times 10^4$ µm K), and T is the absolute temperature (in K).

This equation describes the spectral exitance distribution of a blackbody at a certain temperature as a smooth curve with a single maximum (Figure 2.5). Planck's equation indicates that any object hotter than absolute zero (–273°C) emits radiant energy and that the energy increases in proportion to its temperature. As shown in Figure 2.5, with increasing temperature, an object will radiate more energy and with higher exitance in shorter wavelengths.

The total radiant energy per unit surface area is a function of the object's temperature. The value can be obtained by integrating the spectral radiant exitance over all wavelengths. This is known as the Stefan–Boltzmann law:

$$M_n = \sigma T^4 \tag{2.9}$$

where σ is the Stefan–Boltzmann constant (5.67×10^{-8} W m^{-2} K^{-4}) and T is the temperature in kelvin.

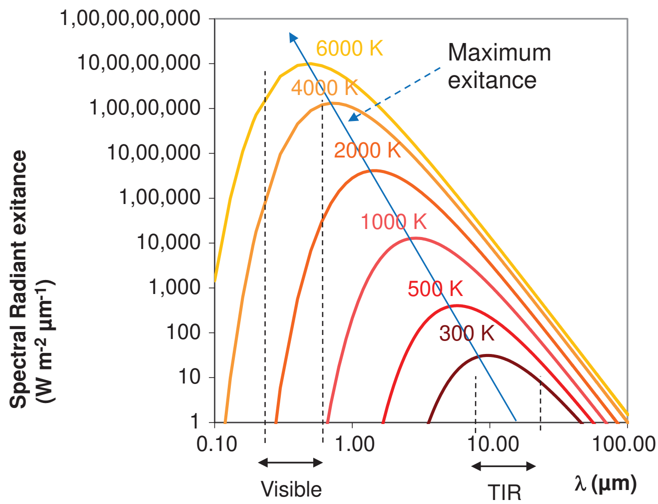

FIGURE 2.5 Blackbody spectral radiant exitance curves at various temperatures.

As M_n is the fourth power of T, small changes in temperature result in large variations in radiant exitance.

Kirchhoff's law enables us to extend the foregoing relationships describing blackbody emission behavior to naturally emitting surfaces through an emissivity (ε) correction:

$$M = \varepsilon \sigma T^4 \quad (2.10)$$

A blackbody is a perfect emitter in that it absorbs and emits all the energy it receives. When an object does not absorb any of the incident energy, it is called a white body, completely reflecting all energy received (emissivity = 0). Gray bodies absorb and emit a fixed proportion of energy equally at all wavelengths. Most objects in nature have emissivity values that vary with wavelength and are referred to as *selective radiators*. Section 6.8.3 presents the methods to convert the thermal radiation M_λ, measured by a sensor, into the surface temperature T. The behavior of emissivity values with wavelength provides a mechanism for the discrimination of surface materials in the TIR.

The single maximum or wavelength of peak spectral radiant exitance of a blackbody may be derived from the first derivative of Planck's radiation law (Equation 2.8), described by Wien's displacement law:

$$\lambda_{max} = \frac{2{,}898\ \mu\text{m K}}{T} \quad (2.11)$$

with the temperature (K) in kelvin. Wien's displacement law is useful to determine the most sensitive band in the EM spectrum for the detection of a certain feature with high thermal contrast with their surroundings. For instance, a forest fire burning at 800–1,000 K would be better detected between 3.6 and 2.98 µm (MIR region).

In summary, the amount and spectral distribution of energy radiated by an object vary according to (1) the temperature of the object and (2) the nature of the material, as depicted by its emissivity. From Equations 2.4 through 2.11, we can estimate the total spectral distribution and radiant exitance of an object by knowing its absolute temperature and emissivity. As with blackbodies, the energy emitted from a natural object is primarily a function of its temperature, but with important modifications dependent on its emissivity. Finally, knowing the temperature and emissivity of an object or surface allows us to determine the most suitable portion of the spectrum for optimal detection and discrimination.

In the following sections, we explore the behavior of EM radiation in more detail by focusing on the three regions of the spectrum where remote sensing measurements are made, namely, the solar spectrum (from VIS to SWIR), the TIR, and the MW portion of the spectrum. Our main interest from an environmental perspective is to better understand how the energy interacts with the main components of the Earth's surface: vegetation, water, soils, snow, and so on. Since these interactions do not occur in vacuum but are rather affected by atmospheric components, we will close this chapter by presenting the main effects of the atmosphere on the detected signal.

2.5 SPECTRAL SIGNATURES IN THE SOLAR SPECTRUM

2.5.1 Introduction

As previously mentioned, the Sun is the main source of EM energy. It is a gaseous body made up mostly of hydrogen. The internal temperature may reach 20 million K, but externally only the surface, called photosphere, is observable. The photosphere is at a temperature of ~6,000 K. Using radiation laws, we can calculate that most of the solar radiant exitance extends over a wavelength range from 0.3 to 3 μm, with a maximum output in the VIS region (0.4–0.7 μm) and peak exitance at 0.50 μm (Figure 2.5).

The actual solar radiation arriving at the top of the Earth's atmosphere (ToA solar irradiance or $E_{0,\lambda}$) is a function of the Sun's temperature, the size of the Sun, and the distance between the Sun and the Earth, and it can be computed as follows:

$$E_{0,\lambda} = M_{6,000,\lambda} \frac{R^2}{D^2} \tag{2.12}$$

where R is the radius of the Sun (6.96×10^5 km), and D is the distance between the Sun and the Earth. D changes throughout the year, following the elliptical orbit of the Earth. The average values can be approximated to 149.6×10^6 km. For this reason, even though the Sun's radiation is always greater than the Earth's (as the Sun is much hotter), the actual solar radiation arriving on Earth is only relevant in the 0.4–2.5 μm band, which is consequently named the solar spectrum (Figure 2.6). For longer wavelengths, radiant exitance from the Earth or from hotter objects is higher than that

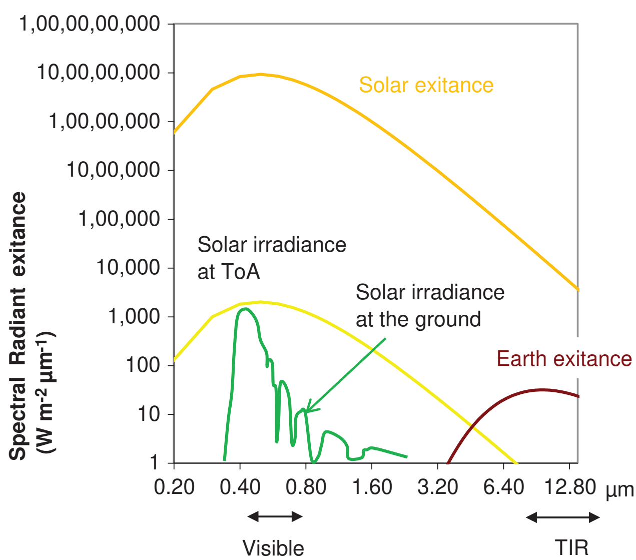

FIGURE 2.6 Solar emittance and Sun irradiance at ToA and at the ground versus Earth's emittance.

from solar radiation. The Earth's surface has an internal temperature of 300 K with a maximum emittance in the 8–14 µm band (TIR) and a peak spectral exitance output at 10 µm.

Average annual solar irradiance (radiation arriving at the top of the atmosphere) is roughly 1361 W m^{-2}, but this amount varies largely throughout the Earth's surface as a function of latitude, day of the year, and time of the day. The actual solar irradiance reaching the ground is always lower than E_0 since the gases and aerosols of the atmosphere filter out different parts of the spectrum (Figure 2.6). Spectral regions where atmospheric transparency is high are called atmospheric windows. Most remote sensing missions include sensors sensitive to those wavelengths as they try to observe the ground. However, when they try to detect atmospheric components, such as ozone, CO_2 concentrations, or water vapor, sensors on board are precisely sensitive to those regions where absorption of that target atmospheric component is more intense.

Solar radiation reaching the ground interacts with different land covers (soils, water, vegetation, asphalt, etc.). The incoming irradiance energy (ϕ_i) will be either reflected (ϕ_r), absorbed (ϕ_a), or transmitted (ϕ_t) by the cover elements (Figure 2.7), and therefore, we can state

$$\phi_i = \phi_r + \phi_a + \phi_t \tag{2.13}$$

or expressed in terms of radiance (W m^{-2} sr^{-1}):

$$L_i = L_r + L_a + L_t \tag{2.14}$$

We can also express these quantities in relative terms by dividing each of the radiances by the incident energy L_i:

$$\frac{L_i}{L_i} = \frac{L_r}{L_i} + \frac{L_a}{L_i} + \frac{L_t}{L_i} \tag{2.15}$$

which becomes

$$1 = \rho + \alpha + \tau \tag{2.16}$$

For any given surface, the magnitudes of the three components are not constant and will vary with wavelength. It is therefore more appropriate to express Equation 2.16 as wavelength dependent:

$$1 = \rho_\lambda + \alpha_\lambda + \tau_\lambda \tag{2.17}$$

The proportions of incident energy that are reflected, absorbed, and transmitted are a function of the unique characteristics of the surface, and these proportions vary with wavelength. In fact, the manner in which solar radiation interacts with the Earth's surface results in variations of the three

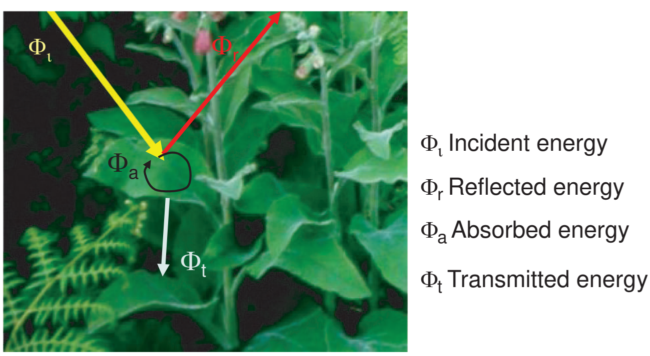

FIGURE 2.7 Interactions of EM energy with the Earth's covers.

components with wavelength, which can tell us much about the chemical and physical properties of the surface. For example, a leaf will appear green if its reflectance at green wavelengths is greater than its reflectance in the blue or red portions of the VIS spectrum. An object will appear blue if it reflects more energy in the blue region than in the green or red spectral bands. In the VIS part of the spectrum, the variation in reflectance behavior of an object over the VIS wavelengths results in the colors we usually see (even though different versions of color blindness are more extended than ordinarily thought).

The reflectance behavior of an object over various wavelengths of the EM spectrum is commonly referred to as a spectral reflectance signature or just spectral signature. Figure 2.8 includes a series of spectral signatures for various covers. These materials have highly variable spectral signatures. The reflectance of snow is very high in the VIS region (blue, green, red), resulting in its "white" appearance (i.e., color theory tells us that high and equal amounts of blue, green, and red result in the color white). As we proceed to longer wavelengths, the reflectance of snow decreases dramatically, and snow appears "dark gray" (near-zero reflectance) over the SWIR wavelengths. Water, on the other hand, has low reflectance in the VIS wavelengths, which decreases toward the NIR and SWIR wavelengths. The presence of sediments, pollutants, phytoplankton, and other constituents, however, alters the spectral signature of water, which allows us to optically and quantitatively measure the amounts and turbidity of the constituents in water. Similarly, dust and pollutants will modify the spectral reflectance signature of snow such that the resulting changes in the remotely sensed spectral signatures can be used to assess the "age" of snow.

Vegetation has unique spectral reflectance signatures with low reflectance in the VIS, high reflectance in the NIR, and low reflectance in the SWIR portion of the spectrum. The spectral signatures of vegetation are modified by leaf type and morphology, leaf physiology, chlorophyll content, plant stress, and senescence. Soils, on the other hand, have spectral reflectance signatures that gradually increase with increasing wavelengths in a manner dependent on their iron, organic matter, water, mineral, and salt content. The spectral signature of a soil will also be modified by its structural and morphologic properties at the surface (e.g., roughness), as well as by the presence of plant litter and its stage of decomposition.

In summary, the relationship between the incident solar energy at the surface and the spectral composition of the remotely sensed reflected energy provides a wealth of information about the biogeochemical nature of the surface (leaf chemistry, soil mineralogy, water content) and the physical and structural characteristics of the surface (e.g., canopy height, leaf area, and soil roughness). The area observed by a sensor will most likely contain a variety of the surface materials

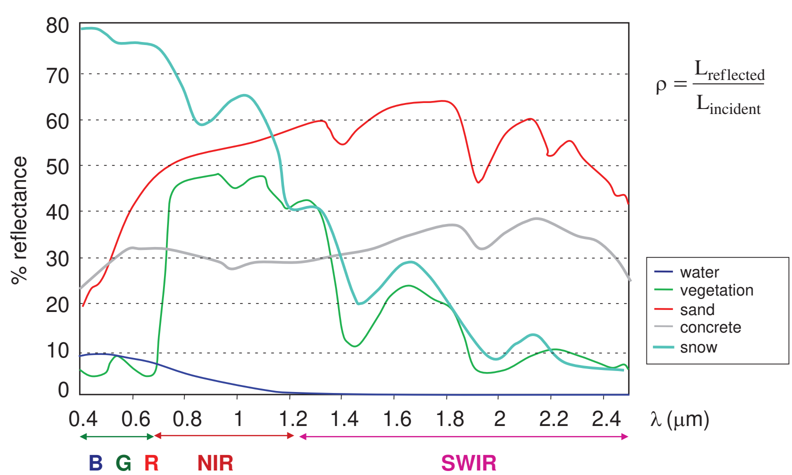

FIGURE 2.8 Spectral reflectance signatures for representative Earth surface materials.

(soil, vegetation, water, litter) in varying proportions and arrangements, and thus, remote sensing measurements often consist of mixed signals comprising multiple reflectance signatures. As we will comment later (see Section 7.1.5), there are various techniques to extract information from these spectral mixings.

Spectral signatures form the basis to discriminate objects from remote sensing measurements in the solar region of the EM spectrum. Unfortunately, these signatures are not constant for each cover, as the radiance flux detected by remote sensing depends not only on the intrinsic properties of the observed area but also on the external conditions of the measurement. The main factors affecting spectral signatures are the following (Figure 2.9):

i. Atmospheric components, which affect both the absorption and the scattering of incoming and reflected radiations.
ii. Land cover variations causing changes in chemical or physical composition, such as density, pigment contents, moisture, or roughness. They may be caused by vegetation or crop phenology, agricultural practices, grazing, etc.
iii. Soil and geologic substrate, which are particularly important in open and sparse canopy covers, as the sensor will detect a stronger signal coming from the background.
iv. Solar illumination conditions, which depend on the latitude, day of the year, and hour of the day.
v. Terrain slope.
vi. Aspect, both affecting the illumination conditions of a target cover.

Among these factors, it is particularly relevant to consider the impact of the geometric conditions of the observation, in particular, the incidence and viewing angles relative to the reflecting surface. This geometric relationship, along with the surface properties (primarily roughness), determines how the incoming radiation is scattered and the strength of the outgoing radiation. There are three

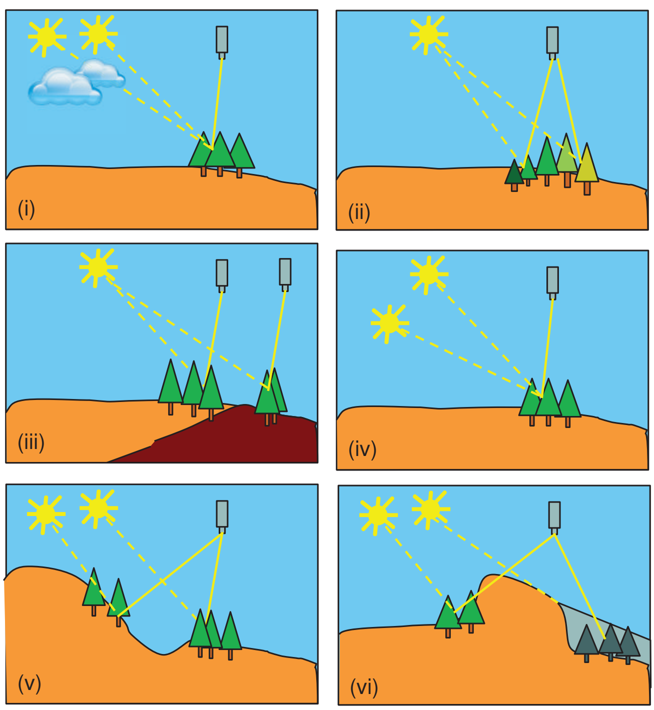

FIGURE 2.9 Factors (see the text) influencing spectral signatures.

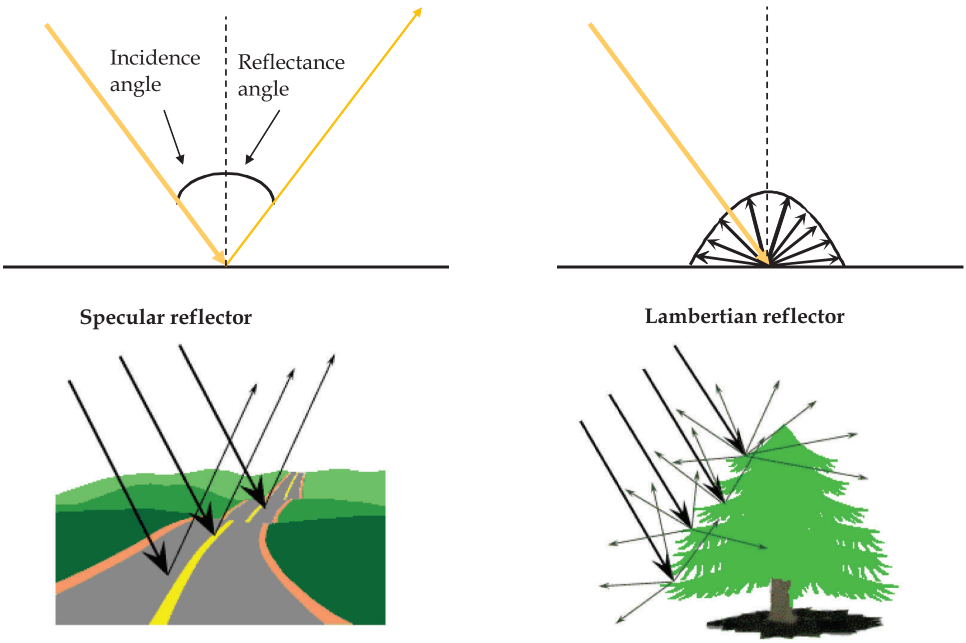

FIGURE 2.10 Major types of surface reflection over a variety of surface roughness conditions.

types of surface scattering that may occur (Figure 2.10). The first type of scattering is known as specular reflection. In specular reflection, surface incident energy is reflected away from the Sun and at the same angle as the solar incident angle, and no energy is scattered in any other direction. In this case, the sensor can measure only the ground reflected energy at this particular viewing angle and will receive no energy at any other viewing directions. In the second type of surface scattering, the incident energy is reflected diffusely and equally, or isotropically, in all directions. When a surface is perfectly diffuse and exhibits the same reflected radiance for any angle of reflection, that is, independent of viewing angle to the surface normal, it is known as a Lambertian surface. Most surfaces exhibit the third type of scattering behavior, known as anisotropic reflectance, in which both diffuse and specular scattering occur.

These factors illustrate some of the challenges involved in the accurate assessment and characterization of land surface conditions with remote sensing data. Therefore, the spectral reflectance signatures presented in Figure 2.8 may be regarded just as reference signatures. In other words, land surface cover types will unlikely have the same observed reflectances as those referred to in their expected spectral signatures. Rather, they show spectral variability caused by surface, illumination, and atmospheric variations, often making it difficult to unequivocally discriminate objects based solely on detected reflectance. Therefore, to obtain sound retrievals from remote sensing images, the interpreter needs to introduce different corrections aiming to remove the influences of those factors. As we will see in Chapter 6, different quantitative methods are available to eliminate or at least mitigate the impact of atmospheric, illumination, and terrain effects.

Despite this, the reference spectral reflectance signatures are very useful in understanding the images and can also be used to select the optimal bands or band combinations for discriminating certain surface properties, as well as to suggest technical requirements for future remote sensing missions.

In the following sections, we analyze in greater detail the spectral behavior and signatures of typical land surface components, namely, vegetation, soil, and water. We discuss the optical properties of these materials and relate their spectral signatures to key biochemical and mineralogical components.

2.5.2 Vegetation Reflectance

The spectral properties and characterization of vegetation canopies are one of the most important and challenging problems in remote sensing. The reflectance properties of a vegetation canopy are complex and a result of many biochemical and biophysical canopy attributes and the external factors that influence the signal detected at the sensor. A complete understanding of the reflectance behavior of a vegetation canopy includes the role of leaf biochemical, plant physiologic, and canopy structural and morphologic properties. Leaf biochemical constituents include pigments, lignins, and water. Differences in pigment concentrations are responsible for "color" changes, primarily in the VIS portion of the spectrum, while leaf MC involves energy interactions in the SWIR portion of the spectrum. Plant physiologic conditions (vigor, phenology, stress) involve nutrient, water, and light availability, which alters the pigments, lignin, and water-related biochemical interactions and affects plant structure. One must also consider the structural properties at the canopy level, which include the leaf area index (LAI), leaf angle distribution (LAD), fractional vegetation cover, plant height, crown diameter, leaf clumpiness, planting geometry, and associations with other species of shrubs, trees, and grasses.

Typically, many of these vegetation properties change simultaneously with plant canopy development, making it difficult to isolate the variation of specific vegetation biophysical components. For example, as a canopy develops, both fractional vegetation cover and LAI change simultaneously, along with pigment and water contents. Aside from the vegetation canopy itself, there is also the underlying background consisting of soil, rock, litter, water, and snow, with optical properties that modify the signal of the overlying vegetation canopy. In addition, a second canopy vegetation layer may be present (shrubs and trees), thus further complicating the retrieval of vegetation parameters. Finally, external to the canopy are also the various influences that alter the signal at the sensor, including Sun illumination and sensor view angles, landscape topography (slope, aspect), and atmospheric effects.

In this section, we introduce some of the most basic vegetation reflectance properties in the solar spectrum. More rigorous treatments involving laboratory-based studies of leaf reflectance, optical–geometric models of plant canopies, and numerical canopy radiative transfer models (RTM) can be found elsewhere (Asner 1998; Asner et al. 2000; Colwell 1974; Gates et al. 1965; Jacquemoud 1990; Jacquemoud et al. 1995; Knipling 1970; Liang 2004; Westman et al. 1988).

The reflectance of a leaf is mostly related to the levels of photosynthetic pigments and leaf water, as well as the leaf's structural characteristics. The overall spectral signature of a leaf or plant is further affected by leaf age, nutrient stress, and health (disease, vigor, etc.). A typical spectral reflectance signature of a green leaf obtained from laboratory measurements is shown in Figure 2.11. There are three main spectral domains influencing the optical properties of leaves, namely, the VIS, the NIR, and the SWIR regions.

The low reflectance in the VIS region (0.4–0.7 μm) is due to the absorbing effect of leaf pigments, mainly chlorophyll a, chlorophyll b, carotenoids, and xanthophylls, with the chlorophyll pigments accounting for 60%–75% of the energy absorbed (Gates et al. 1965). All of these pigments absorb in the "blue" region of the EM spectrum centered on wavelengths ~0.45 μm, while chlorophyll also absorbs in the "red" portion of the spectrum, centered on ~0.65 μm. Between the blue and red spectral regions, there is a spectral region of less intensely absorbed radiation, a "green reflectance peak" at 0.55 μm, which is responsible for the green appearance of healthy leaves. Because energy in the 0.4–0.7 μm range is absorbed by pigments to drive photosynthesis, the term "incident photosynthetically active radiation" (IPAR) is often used to describe the radiation in the VIS part of the spectrum.

Other pigments also have an important effect on the spectral reflectance of leaves in the VIS spectrum. For example, the yellow to orange-red pigment carotene has a strong absorption in the 0.35–0.50 μm range and is responsible for the color of some flowers and fruits as well as leaves without chlorophyll. When leaves undergo senescence, chlorophyll levels and the associated absorptance

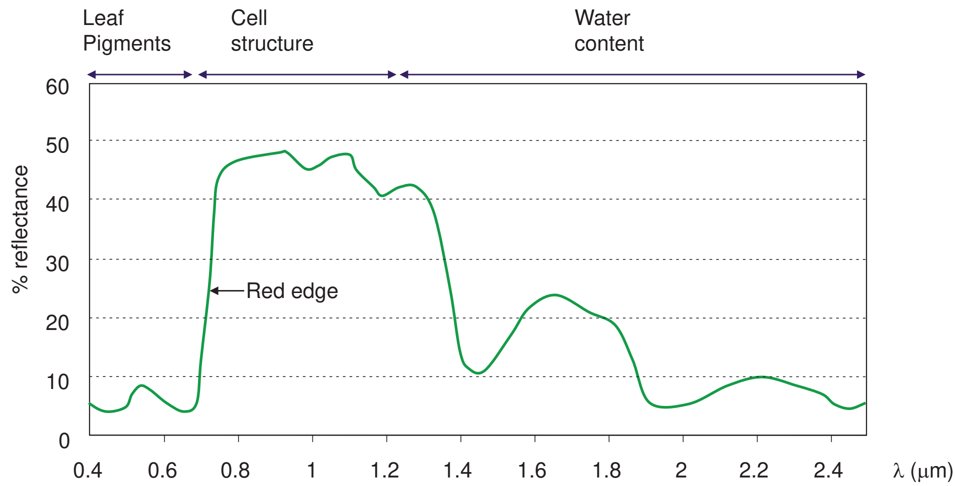

FIGURE 2.11 Green leaf spectral reflectance.

decrease, causing a higher red reflectance, which combined with the green reflectance yields a yellowish color (green + red = yellow). The influence of the more persistent carotenoid pigments becomes more pronounced as the amount of chlorophyll in the leaves decreases during senescence. In some species, the red and blue pigment xanthophyll with strong absorption at 0.35–0.50 μm becomes prominent with leaf aging, resulting in many of the leaf colors in autumn (e.g., northern maples and Chilean Nothofagus).

Beyond the highly absorbing red region is the sharp "red edge" transition region at ~0.74–0.78 μm, in which leaf pigments and cellulose become transparent to NIR wavelengths. Leaves have very low absorptance in the NIR band (<10%) and high leaf reflectance that can reach 50%. Plant nutrient and mineral stresses are known to cause shifts in the red edge. The region between 0.70 and 1.1 μm is called the NIR reflectance plateau, where reflectance is high, except in two minor water-related absorption bands (0.96 and 1.1 μm), which depend on the internal cellular structure of the leaf.

Leaf structural properties strongly influence reflectance, particularly by the relative thickness of the mesophyll cell layer. The spongy mesophyll layer contains internal air cavities that scatter incident radiation (Figure 2.12). Leaf reflectance increases for more heterogeneous cell shapes

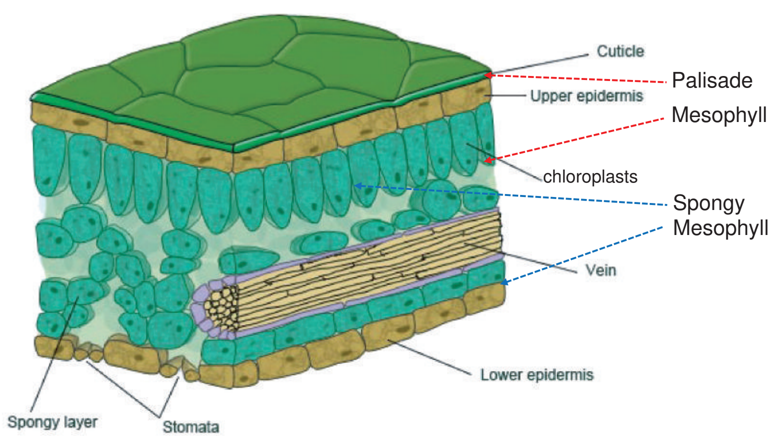

FIGURE 2.12 Basic components and cellular structure of a leaf. (Adapted from http://igbiologyy.blogspot.com.es/2013/01/46-leaf-structure.html)

and contents as well as with increases in the number of cell layers, intercellular spaces, and variations in cell size. The vegetation spectral reflectance curves are modified by the morphology of the leaf. Thus, needle leaves tend to exhibit greater absorptance across all wavelengths, while desert succulent plants will reflect more energy than other mesophytic species (Gates et al. 1965). As a result of NIR sensitivity to leaf structural properties, which varies across plant species, the NIR spectral region is very useful in plant biodiversity studies and in discriminating among plant species that are often not distinguishable in the VIS spectrum.

The NIR spectral domain also has a transition area between 1.1 and 1.3 μm, where reflectance decreases sharply from the NIR reflectance plateau to the low-reflecting SWIR domain (1.3–2.5 μm) (Figure 2.12). This region is characterized by strong absorption by leaf water. Leaf water strongly absorbs incident solar radiation in this range but is transparent to the shorter VIS or IPAR wavelengths. Reflectance of SWIR wavelengths generally increases as leaf liquid water content decreases; however, water absorbs radiation so strongly at 1.45 and 1.95 μm that these wavelengths cannot be used in land remote sensing because most of the solar radiation in these wavelengths is absorbed by the atmosphere before reaching the ground.

From laboratory measurements, we see dramatic differences between dry leaves and leaves infiltrated with water in this spectral region, especially at wavelengths near 1.45, 1.92, and 2.7 μm (Lusch 1989; Short 1982; Yebra et al. 2013a: Figure 2.13), although these variations depend on the leaf type and plant species (Westman and Price 1988). A sensor placed above a canopy does not measure individual leaves but rather many leaves forming the vegetation canopy. The overall radiation transferred through the canopy also depends on the structural arrangement and quantity of leaves within a canopy. The canopy's structural or optical–geometric properties include canopy architecture, LAD, LAI, ground cover fraction, leaf "clumping," species composition, leaf morphology, leaf size and shape, and the underlying soil and litter.

In spite of this structural complexity, there are many common features in most vegetation spectra, such as the high contrast observed between the R band (~0.645 μm) and the NIR region (0.7–1.3 μm). In general, one can say that the greater the contrast between these two regions, the greater the amount and vigor of the vegetation. This theoretical spectral behavior of vegetation in the R and NIR forms the basis for the design and development of vegetation indices (see Section 7.1.3). Vegetation indices are constructed from combinations of these two bands when multispectral images are available. They are designed to isolate and enhance the vegetation signal in remotely sensed imagery, thereby facilitating the discrimination and extraction of useful vegetation information (Asrar et al. 1992; Gutman 1991; Huete et al. 1994; Huete et al. 1997).

It is implicit that any source of stress in the vegetation will cause a change in its spectral behavior. Senescent or stressed leaves tend to immediately reduce chlorophyll activity, resulting in less

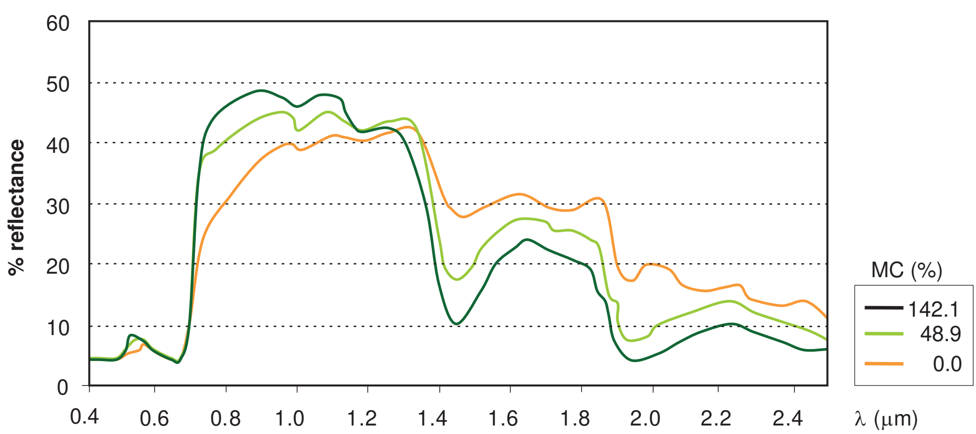

FIGURE 2.13 Leaf spectral signatures as a function of MC, estimated as water weight over leaf dry weight.

absorptance in the red band, with slight decreases in blue absorption (since carotenes persist and continue to absorb in the blue). The consequent increase in R reflectance and the slight increase in B reflectance alter the proportion of reflectance in the primary colors (B, G, R), resulting in a change in leaf color. This is why leaves tend to show a yellowish color with senescence or stress. Stress may also reduce leaf reflectance in the NIR portion of the spectrum, due to the deterioration of the cellular structure of the leaf. The spectral curve often becomes flatter and less chromatic (Knipling 1970; Murtha 1978).

Such information is valuable in detecting damages produced by pollution, insects (Rock et al. 1986; Souza et al. 2005), or fires (Chuvieco et al. 2019). The contrast between NIR and SWIR has also been extensively used to estimate leaf MC, providing an estimation of other controlling factors is available (Ceccato et al. 2002b; Yebra et al. 2013a). In addition, it has been shown that certain factors in leaf stress are associated with a displacement in the R edge, the slope change in the spectral curve between red and the NIR, toward shorter wavelengths. For instance, this phenomenon has been observed when the plants are affected by heavy metal contamination (Rock et al. 1986).

2.5.3 Soil Reflectance Properties

Much is known about soil properties through extensive laboratory and in situ field measurements. In contrast to vegetation, very little EM energy is transmitted through soils, and therefore, their spectral signature is basically related to the most superficial conditions. The spectral composition of energy reflected and emitted by soil is mostly dependent on the biogeochemical (mineral and organic) constituents, optical–geometrical scattering properties (particle size, aspect, roughness), and moisture conditions of the immediate soil surface (Ben-Dor et al. 2008; Lusch 1989; Mulders 1987). For example, soils with high quartz content often reflect a large portion of incoming energy across the EM spectrum, and wet soils absorb most of the NIR and SWIR light they receive, while soils with high organic matter tend to absorb much of the incoming VIS light.

Different soil spectral reflectance signatures result from the presence or absence, as well as the position and shape of specific absorption features, of a number of soil constituents. Absorption is due to various chemical/physical phenomena such as intermolecular vibrations and electronic processes in atoms. The VIS–NIR regions (0.4–1.1 µm) contain broad spectral absorption features such as strong absorption near 1 µm due to ferrous iron, with weaker absorptions at 0.7 and 0.87 µm. Strong Fe–O charge transfers in the blue and ultraviolet region result in fairly steep decreases in reflectance with shorter wavelengths. Iron is fairly ubiquitous, so most soils exhibit increasing reflectance with wavelength over the VIS to NIR portion of the spectrum (Mulders 1987).

Soils have distinct spectral features in the SWIR region caused by atomic vibrational processes, which include two broad water absorption bands at 1.4 and 1.9 µm. Minerals with OH, CO_3 (calcite), and SO_4 (gypsum) exhibit absorption features in the 1.8–2.5 µm region, while layer silicates with OH absorb near 1.4 and 2.2 µm (Mulders 1987; Shepherd and Walsh 2002). Humus content also has a great influence on soil color, tending toward a low reflectance, especially around 0.7–0.75 µm (Curran et al. 1990).

Soils are mixtures of a number of inorganic and organic constituents, so it is not straightforward to evaluate the composition of soils from their spectral signatures (Ben-Dor et al. 2008). Many soil spectra signatures are fairly similar, making it difficult to distinguish them. As a result, only a limited number of soil spectral curves have been found to be distinguishable when using remote sensing. Stoner and Baumgardner (1981) analyzed the spectral signatures of a great variety of soils (485 types), from 0.50 to 2.45 µm, and documented five unique soil spectral curve shapes primarily related to their relative contents of organic matter and iron and modulated by their textures. Other spectral libraries, such as the NASA Jet Propulsion Laboratory (JPL) Aster, include a wide range of soil spectral signatures (Figure 2.14). These, along with numerous laboratory and field studies, have shown that soil spectral signatures are largely controlled by the iron oxides, organic molecules, and water that coat soil particles.

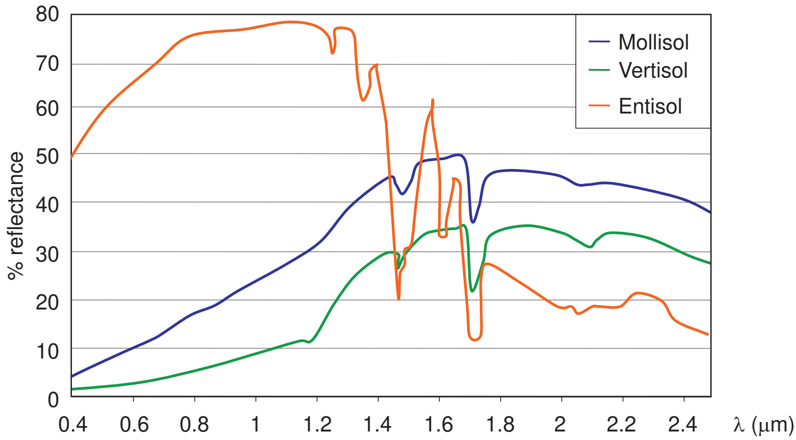

FIGURE 2.14 Spectral reflectance for different soil types: Mollisol (gray silt), Vertisol (brown clay), and Entisol (white gypsum). (From http://speclib.jpl.nasa.gov/)

Most soil surfaces scatter incident radiation anisotropically, which is a consequence of a soil's 3D structure. Scattering takes the form of diffuse and specular reflection and is sensitive to the geometric properties of soil components (particle size, aspect, roughness), the macro soil surface, sensor viewing angle, solar illumination angle, and the relative azimuthal positions of the Sun and sensor relative to the surface (Ben-Dor et al. 2008; Stoner and Baumgardner 1981). With the shortest wavelengths most affected, roughness and Sun–soil–sensor geometries alter a soil's spectral signature and the inferences of basic soil properties such as soil mineralogy. Remote sensing data taken under different Sun and viewing geometries are not necessarily comparable without correction for these angular effects (see Section 6.8.2.4).

Particle size distribution and surface height variation (roughness) are the most important factors influencing the directional reflectance of bare soils. They cause a decrease in reflectance with increasing size of "roughness elements" as coarse aggregates contain many inter-aggregate spaces and "light traps." Smooth, crusted, compacted, and structureless soils generally reflect more energy and are brighter (Lusch 1989). Clayey soils, despite having a finer particle size distribution, tend to be darker than sandy soils because clays aggregate and behave as larger, "rougher" surfaces.

Soil moisture has a strong influence on the amount and composition of reflected and emitted energy from a soil surface, and thus, information about soil moisture condition can be derived from measurements in all parts of the EM spectrum. In the shortwave region, the major effect of adsorbed water on soil reflectance is a pronounced decrease in reflected energy, making soils darker when moistened, particularly in the water absorption bands centered at 1.45 and 1.9 μm (Reginato et al. 1977). The decrease in reflectance is proportional to the thickness of the water film around the soil particles and can be related to the gravimetric water content as well as energy status of the adsorbed water.

In the shortwave portion of the spectrum, the SWIR region is considered most sensitive to surface MC. Water absorption in these two bands can be expressed as a ratio, relative to the other bands, or in linear combination and then related to soil water content for discrete soil textural classes.

At the landscape level, it is much more difficult to measure soil properties and extract soil information with space-borne sensors. This is due to the extreme spatial variability of soil properties and because the soil surface is often masked by vegetation and plant litter. The discrimination and mapping of soil types and soil properties becomes a function of not only the properties of the surface materials but also sensor characteristics such as number of wavebands, bandwidths, spatial resolution, and instrument noise. The wealth of knowledge available from laboratory, field, and model studies, however, provides a strong foundation and starting point for the extraction of soil information at the more heterogeneous landscape level.